Tight Bounds for Uncertain Time-Correlated Errors With Gauss–Markov Structure in Kalman Filtering

OMAR GARCÍA CRESPILLO, Member, IEEE
German Aerospace Center (DLR), Oberpfaffenhofen, Germany

STEVE LANGEL
The MITRE Corporation, McLean, VA USA

MATHIEU JOERGER, Senior Member, IEEE
Virginia Tech, Blacksburg, VA USA

Safety-critical navigation applications require that estimation errors be reliably quantified and bounded. This can be challenging for linear dynamic systems if the process noise or measurement errors have uncertain time correlation. In many systems (e.g., in satellite-based or inertial navigation systems), there are sources of time-correlated sensor errors that can be well modeled using Gauss–Markov processes (GMP). However, uncertainty in the GMP parameters, particularly in the correlation time constant, can cause misleading error bounds. In this article, we develop time-correlated models that ensure tight upper bounds on the estimation error variance, assuming that the actual error is a stationary first-order GMP with a variance and time constant that are only known to reside within an interval. We first use frequency-domain analysis to derive stationary GMP models in both the continuous and discrete-time domains, which outperform models previously described in the literature. Then, we derive an even tighter estimation error bound using a nonstationary GMP model, for which we determine the minimum initial variance that guarantees bounding conditions. Both models can easily be implemented in a linear estimator like the Kalman filter.

Manuscript received 10 June 2022; revised 24 November 2022; accepted 24 January 2023. Date of publication 7 February 2023; date of current version 9 August 2023.

DOI. No. 10.1109/TAES.2023.3242943

Refereeing of this contribution was handled by J. Blanch. *(Corresponding author: Omar García Crespillo.)*

Authors' addresses: Omar García Crespillo is with the Navigation Department of the German Aerospace Center (DLR), 82234 Oberpfaffenhofen, Germany, E-mail: (Omar.GarciaCrespillo@dlr.de); Steve Langel is with the Department of Comms, SIGINT, and PNT, The MITRE Corporation, McLean, VA 20151-3707 USA, E-mail: (slangel@mitre.org); Mathieu Joerger is with the Kevin T. Crofton Department of Aerospace and Ocean Engineering, Virginia Tech, Blacksburg, VA 24061 USA, E-mail: (joerger@vt.edu).

I. INTRODUCTION

Safety and liability-critical applications require a guaranteed bound on the estimation error, even when process and measurement noise cannot be precisely characterized. The concept of cumulative distribution function (CDF) overbounding supports safe error quantification in the context of global navigation satellite systems (GNSS) positioning [1], [2]. However, CDF overbounding is designed to be used only for snapshot estimators, such as least-squares estimators [3], [4], [5]. That is, it does not directly apply to linear dynamic systems (LDSs) because it does not account for measurement error correlation *over time*. New navigation applications are emerging that require the use of Kalman filters (KFs) or other sequential or fixed-lag estimators to meet stringent requirements and to incorporate information from other sensors e.g., from inertial navigation systems (INS).

Robust estimation approaches have been developed to address model uncertainty in LDSs. For instance, the optimization of a scaling parameter to bound the estimation error using a discrete-time KF is proposed in [6]. This approach can present limitations due to the need to perform an optimization process at each time step, and it only considers uncertainty in the process and measurement design matrices, not in the noise terms that are of main interest in this article. In [7], the authors also aim at guaranteed cost filtering under system uncertainty, but noise structure uncertainty is not considered. Other robust filters use norm-bounded cost functions based on $H\infty$ or $H2/H\infty$ [8], [9] or use cost functions based on M-estimators [10]. They have been implemented in navigation applications and show great potential [11]. But, they do not allow for rigorous estimation error bounding, which makes them unfit for safety-critical applications.

The authors in [12] and [13] provide bounds on the error of linear systems with spherically symmetric time correlated measurement errors. In [14], a bounding approach is proposed when the autocorrelation function of measurement or process noise can be upper and lower bounded. While these methods do not require any knowledge about the structure of the errors, they require evaluating the impact of all previous time epochs in a batch processing scheme. This is a limitation for real-time systems since the required operations and memory allocation grow fast as time passes. In [15], the authors show that the true KF estimation error covariance could be upper bounded if the power spectral density (PSD) of the measurement or process error model upper bounded that of the actual time-correlated sensor errors at all frequencies.

Realistic time-correlated errors can have complex time correlation structures. To model these structures in practical applications, Gauss–Markov Processes (GMPs) are widely employed both because they can be reasonably accurate and have a simple two-parameter formulation. GMPs can easily be incorporated in a KF by state augmentation. For instance, the satellite-based augmentation system minimum operational performance standard recommends using first-order GMP to model the tropospheric, satellite ephemeris, and clock errors in GPS/INS tight integration [16]. However, time-correlated errors that can be considered stationary over the duration of a Kalman filtering period may change over longer time scales, and may vary depending on sensor location. This has been observed, for instance, in GNSS satellite orbit and clock errors, residual tropospheric delays, and multipath errors; in these cases, ranges of values for GMP variance and time-constant are provided [17], [18], [19]. Error models are needed, which incorporate the fact that true process parameters are uncertain, thereby enabling realistic predictions of estimator performance in the presence of time correlation. Such models have begun to emerge in the literature. In [20], a stationary model for uncertain GMPs is derived by sensitivity analysis of continuous-time KFs. This derivation is revisited for sampled-data systems in [21] and a tighter, nonstationary model is provided in the discrete-time domain. However, Langel et al. [21] does not prove that the model guarantees an upper bound on the estimate error variance. In [22], the model from [21] is implemented in a GNSS/INS KF for an aircraft landing application: the authors conjectured that another model may exist that can provide a tighter bound on the KF estimate error variance. Langel et al. [23] provided rigorous proofs that the models in [21] are bounding, and these models are applied to a batch ARAIM application. Thus, while prior work in [20], [21], and [23] guarantee an upper bound on estimation error variance, they are not designed to achieve any measure of optimality. In this article, we derive a closed-form solution for the tightest stationary GMP model that upper bounds the KF estimate error variance in the presence of measurement and process noise with stationary GMP structure but uncertain variance and time constant. Both continuous and discrete-time models are found using the PSD criterion in [15]. These bounds not only guarantee bounding error conditions but also provide smaller predicted KF error covariances with respect to previous work in [20], [21], and [23]. In safety-critical applications, they can be used to ensure integrity while enhancing continuity and availability performance. Then, we tighten the discrete implementation of the bound by considering a nonstationary GMP model whose initial variance is less than the steady-state variance. The nonstationary bound is tighter during the transient phase of the nonstationary process, and remains bounding at steady state.

The rest of this article is organized as follows. In Section II, we derive the parameters of a stationary GMP bound in the continuous-time domain and represent its PSD. In Section III, we present the stationary GMP model derived in the discrete-time domain. Sections IV and V provide nonstationary bounding models for the continuous and discrete-time domain, respectively, by deriving conditions on the initial GMP variance. A reader only interested in applying the new bounds may directly consult Table I in Section VI. In Section VII, we evaluate the bounds for an example KF implementation. Finally, Section VIII concludes this article.

II. STATIONARY CONTINUOUS-TIME GMP MODEL

A. Problem Formulation

We consider a hybrid LDS described by a continuous-time system model and a sampled measurement model at a time epoch $n \in \mathbb{Z} \geq 0$:

$$\dot{\boldsymbol{\xi}}(t) = \mathbf{F}(t)\boldsymbol{\xi}(t) + \mathbf{w}(t),$$
$$\mathbf{z}_n = \mathbf{H}_n\boldsymbol{\xi}_n + \mathbf{v}_n, \tag{1}$$

where $\mathbf{F}$ and $\mathbf{H}$, respectively, are the state transition and observation matrices, and $\boldsymbol{\xi}$ and $\mathbf{z}$ are the state and measurement vectors. A hybrid LDS is a common state-space realization in GNSS/INS. Vectors $\mathbf{w}(t)$ and $\mathbf{v}_n$ are time-correlated process and measurement noise vectors such that

$$\mathbf{w}(t) = \mathbf{E}_{\rm w}\mathbf{a}(t) + \boldsymbol{\eta}(t), \tag{2}$$
$$\mathbf{v}_n = \mathbf{E}_{\rm v}\mathbf{a}_n + \boldsymbol{\nu}_n, \tag{3}$$

where $\mathbf{E}_{\rm w}$ and $\mathbf{E}_{\rm v}$ are matrices of 0s and 1s and $\boldsymbol{\eta}(t)$, $\boldsymbol{\nu}_n$ are mutually uncorrelated, zero-mean white Gaussian noise vectors. $\mathbf{a}_n$ is the sampled signal $\mathbf{a}(t)$ such that $\mathbf{a}_n = \mathbf{a}(n\Delta t)$, where $\Delta t \in \mathbb{R}_{>0}$ is the sampling interval. The $l \times 1$ vector $\mathbf{a}$ is composed of mutually independent stationary first-order GMPs. Each GMP i is modeled by the following differential equation [24]:

$$\dot{a}_i(t) = -\frac{1}{\tau_i}a_i(t) + \sqrt{\frac{2\sigma_i^2}{\tau_i}}\zeta_i(t),\ \ \zeta_i(t) \sim \mathcal{N}(0, 1), \tag{4}$$

or equivalently in vector form

$$\dot{\mathbf{a}}(t) = \mathbf{L}\mathbf{a}(t) + \mathbf{u}(t), \tag{5}$$

where

$$\mathbf{L} = \text{diag}\left[-\frac{1}{\tau_1}, \ldots, -\frac{1}{\tau_l}\right], \tag{6}$$

$$\mathbf{U} = E[\mathbf{u}\mathbf{u}^T] = \text{diag}\left[\frac{2\sigma_1^2}{\tau_1}, \ldots, \frac{2\sigma_l^2}{\tau_l}\right], \tag{7}$$

where $\tau_i \in \mathbb{R}_{>0}$ and $\sigma_i^2 \in \mathbb{R}_{\geq 0}$ are the GMP correlation time constant and variance, respectively, with $i \in 1, \ldots, l$ and $\mathbf{u}(t)$ is a zero-mean white Gaussian noise vector. The condition $\tau_i > 0$ ensures that the system in (5) is stable. We only consider stable GMPs since most random processes encountered in practice exhibit this behavior. Since (1) to (5) define a linear system driven by zero-mean white Gaussian noise, and the KF is a linear unbiased estimator, error bounding conditions can be derived by focusing solely on the estimate error covariance. Under the mutually independent GMP assumption, the bounding methodology in [15] and [23] can be implemented for each GMP separately. We drop subscripts i in the rest of this article when referring to an arbitrary GMP's parameters.

The state-augmented model of the LDS in (1) can be written as

$$\begin{bmatrix}\dot{\boldsymbol{\xi}}(t)\\ \dot{\mathbf{a}}(t)\end{bmatrix} = \begin{bmatrix}\mathbf{F}(t) & \mathbf{E}_{\rm w}\\ \mathbf{0} & \mathbf{L}\end{bmatrix}\begin{bmatrix}\boldsymbol{\xi}(t)\\ \mathbf{a}(t)\end{bmatrix} + \begin{bmatrix}\boldsymbol{\eta}(t)\\ \mathbf{u}(t)\end{bmatrix}, \tag{8}$$

$$\mathbf{z}_n = \begin{bmatrix}\mathbf{H}_n & \mathbf{E}_\mathrm{v}\end{bmatrix}\begin{bmatrix}\boldsymbol{\xi}_n \\ \mathbf{a}_n\end{bmatrix} + \boldsymbol{\nu}_n. \quad (9)$$

In this article, we design a KF to guarantee that the state estimation error covariance matrix tightly upper bounds, in a positive semidefinite sense, the true error covariance matrix when the GMP parameters in **L** and **U** are uncertain within known ranges, i.e., $\tau \in [\tau_\mathrm{min}, \tau_\mathrm{max}]$ and $\sigma^2 \in [\sigma^2_\mathrm{min}, \sigma^2_\mathrm{max}]$. Examples of navigation error sources that can be characterized with a range of parameter values include GNSS satellite orbit, clock, tropospheric, and multipath errors [17], [18], [19].

To model the KF process and measurement noise, we first analyze the PSD, which is a widely used methodology [24]. It was shown in [15] that the KF's estimated state error covariance matrix upper bounds that of the true state error if, for each of the independent process and measurement errors, the model PSDs bound the empirical PSDs. Therefore, we seek to find a GMP model whose PSD upper bounds that of an actual GMP with uncertain time constant and variance. The spectral density of a GMP in the continuous-time domain can be expressed as [24]

$$S_\mathrm{c}(\omega) = \frac{2\sigma^2/\tau}{\omega^2 + (1/\tau)^2}, \quad (10)$$

where the angular frequency in radians per second is $\omega = 2\pi f$, with f being the linear frequency in Hertz. Since the spectrum of a real process is an even function, we only need to bound the PSD over $[0, \infty)$

$$\hat{S}_\mathrm{c}(\omega) \geq S_\mathrm{c}(\omega), \quad \forall\omega \in [0, \infty), \quad (11)$$

where $\hat{S}_\mathrm{c}$ is the bounding PSD of the continuous-time GMP model to be determined.

The bounding GMP model is fully defined by two parameters: its correlation time constant $\hat{\tau}_\mathrm{c} \in \mathbb{R}_{>0}$ and its variance $\hat{\sigma}^2_\mathrm{c} \in \mathbb{R}_{\geq 0}$, which is also the total net power of the GMP process. The KF state estimation error covariance is a linear combination of the variance of the process and measurement noise components. Therefore, in order to find the tightest stationary bound, we want to minimize the total net power of each of the noises, which is expressed for an arbitrary noise as

$$\min_{\hat{\sigma}_\mathrm{c}, \hat{\tau}_\mathrm{c}} \frac{1}{\pi}\int_0^\infty \hat{S}_\mathrm{c}(\omega) d\omega = \min \hat{\sigma}^2_\mathrm{c}, \text{ s.t. } \hat{S}_\mathrm{c}(\omega) \geq S_\mathrm{c}(\omega),$$
$$\forall\omega \in [0, \infty), \forall\tau \in [\tau_\mathrm{min}, \tau_\mathrm{max}] \text{ and } \forall\sigma^2 \in [\sigma^2_\mathrm{min}, \sigma^2_\mathrm{max}]. \quad (12)$$

B. GMP Continuous-Time Model Parameters

The GMP bounding model in the continuous-time domain is presented by the following theorem.

THEOREM 1: Let $a(t) \in \mathbb{R}$ be a continuous-time, stationary, first-order GMP with uncertain variance $\sigma^2 \in [\sigma^2_\mathrm{min}, \sigma^2_\mathrm{max}]$ and correlation time constant $\tau \in [\tau_\mathrm{min}, \tau_\mathrm{max}]$. The correlation time constant and variance of a continuous-time, stationary, first-order GMP model $\hat{a}(t) \in \mathbb{R}$ that provides the tightest bound on the PSD of the process $a(t)$ can, respectively, be expressed as

$$\hat{\tau}_\mathrm{c} = \sqrt{\tau_\mathrm{min}\tau_\mathrm{max}}, \quad \text{and} \quad \hat{\sigma}^2_\mathrm{c} = \sqrt{\frac{\tau_\mathrm{max}}{\tau_\mathrm{min}}}\sigma^2_\mathrm{max}. \quad (13)$$

PROOF: Theorem 1 gives a closed-form solution for the minimization problem in (12). To find this solution, we start by using (10) to express (11) as

$$\frac{2\hat{\sigma}^2_\mathrm{c}/\hat{\tau}_\mathrm{c}}{\omega^2 + 1/\hat{\tau}^2_\mathrm{c}} \geq \frac{2\sigma^2/\tau}{\omega^2 + 1/\tau^2}, \quad \forall\omega \in [0, \infty). \quad (14)$$

Subtracting the right-hand-side term from both sides of the inequality, writing the resulting fraction with a common denominator, and factoring out ω^2 in the terms where it appears in the numerator, (14) becomes

$$\frac{\omega^2(2\hat{\sigma}^2_\mathrm{c}\tau - 2\sigma^2\hat{\tau}_\mathrm{c}) + \frac{2\hat{\sigma}^2_\mathrm{c}\hat{\tau}_\mathrm{c} - 2\sigma^2\tau}{\tau\hat{\tau}_\mathrm{c}}}{\tau\hat{\tau}_\mathrm{c}(\omega^2 + 1/\hat{\tau}^2_\mathrm{c})(\omega^2 + 1/\tau^2)} \geq 0, \quad \forall\omega \in [0, \infty). \quad (15)$$

Since ω, τ, and $\hat{\tau}_\mathrm{c}$ are positive, the denominator in (15) is always positive. Therefore, the numerator must also be nonnegative

$$\omega^2(\hat{\sigma}^2_\mathrm{c}\tau - \sigma^2\hat{\tau}_\mathrm{c}) + \frac{\hat{\sigma}^2_\mathrm{c}\hat{\tau}_\mathrm{c} - \sigma^2\tau}{\tau\hat{\tau}_\mathrm{c}} \geq 0, \quad \forall\omega \in [0, \infty). \quad (16)$$

Equation (16) is linear in ω^2, i.e., monotonically increasing or decreasing with $\omega \geq 0$. Thus, a necessary and sufficient condition for (16) to be satisfied $\forall\,\omega \in [0, \infty)$ is that it must hold true for the two limit values of ω. At the limit when $\omega \to \infty$ and $\omega = 0$, we find the following two conditions:

$$\hat{\sigma}^2_\mathrm{c}\tau - \sigma^2\hat{\tau}_\mathrm{c} \geq 0, \quad (17)$$
$$\hat{\sigma}^2_\mathrm{c}\hat{\tau}_\mathrm{c} - \sigma^2\tau \geq 0, \quad (18)$$

which can be rewritten as

$$\hat{\sigma}^2_\mathrm{c} \geq \frac{\sigma^2\tau}{\hat{\tau}_\mathrm{c}}, \quad \hat{\sigma}^2_\mathrm{c} \geq \frac{\sigma^2\hat{\tau}_\mathrm{c}}{\tau}. \quad (19)$$

These expressions must be satisfied $\forall\tau \in [\tau_\mathrm{min}, \tau_\mathrm{max}]$ and $\forall\sigma^2 \in [\sigma^2_\mathrm{min}, \sigma^2_\mathrm{max}]$. Both conditions are clearly more restrictive when $\sigma^2 = \sigma^2_\mathrm{max}$. The first one is also more restrictive when $\tau = \tau_\mathrm{max}$, whereas the second one is more restrictive when $\tau = \tau_\mathrm{min}$. Thus, when considering the entire range of possible GMP model parameter values, (19) becomes

$$\hat{\sigma}^2_\mathrm{c} \geq \frac{\sigma^2_\mathrm{max}\tau_\mathrm{max}}{\hat{\tau}_\mathrm{c}}, \quad \hat{\sigma}^2_\mathrm{c} \geq \frac{\sigma^2_\mathrm{max}\hat{\tau}_\mathrm{c}}{\tau_\mathrm{min}}. \quad (20)$$

Equation (12) expresses the fact that the tightest GMP bound is the one that minimizes $\hat{\sigma}^2_\mathrm{c}$. In (20), this is achieved at equality, i.e., for the following equations:

$$\hat{\sigma}^2_\mathrm{c} = \frac{\sigma^2_\mathrm{max}\tau_\mathrm{max}}{\hat{\tau}_\mathrm{c}}, \quad \hat{\sigma}^2_\mathrm{c} = \frac{\sigma^2_\mathrm{max}\hat{\tau}_\mathrm{c}}{\tau_\mathrm{min}}. \quad (21)$$

Solving (21) for $\hat{\sigma}^2_\mathrm{c}$ and $\hat{\tau}_\mathrm{c}$ gives (13). This ends the proof for Theorem 1. ■

COROLLARY 1.1 The estimated covariance matrix of a continuous-time LDS estimator (e.g., a KF) whose measurement and process noise are linear combinations of

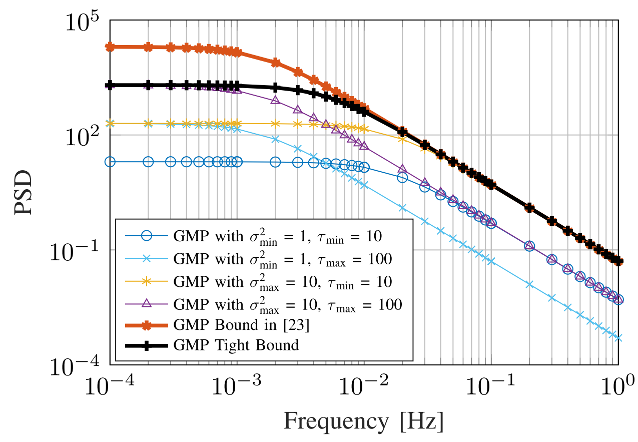

Fig. 1. PSD of stationary GMP with $\sigma^2 \in [1, 10]$ and $\tau \in [10, 100]s$, GMP Bound in [23], and the new Tight Bound.

independent, stationary, first-order GMPs with uncertain parameters $\sigma^2 \in [\sigma^2_{\min}, \sigma^2_{\max}]$ and $\tau \in [\tau_{\min}, \tau_{\max}]$ can be tightly bounded in a positive semidefinite sense by modeling each independent GMP as a continuous-time, stationary, first-order GMP model with parameters given in (13).

PROOF Theorem 1 establishes that the PSD of a GMP model with the parameters given in (13) tightly upper bounds that of a GMP with uncertain parameters $\sigma^2 \in [\sigma^2_{\min}, \sigma^2_{\max}]$ and $\tau \in [\tau_{\min}, \tau_{\max}]$. In addition, Langel et al. [23] proved that, for linear estimators, the state estimation error covariance matrix is bounded if the PSDs of the measurement and process noise models bound those of the actual, independent, time-correlated processes. Therefore, under the assumptions made in this section, designing an LDS estimator (e.g., a KF) using continuous-time GMP models with parameters given in (13) ensures a bounding state estimation error covariance. ∎

C. Graphical Evaluation

We consider an illustrative example of an actual GMP with variance ranging between 1 and 10 (units are arbitrary) and time constant varying from 10 to 100 s. Fig. 1 shows the PSD of the new, tight stationary GMP bound defined in (13) as compared to the stationary bound derived in [21] and [23], and to other possible realizations of the GMP within the admissible range of σ^2 and τ values. Fig. 1 illustrates the fact that our new proposed bound is tighter at low frequencies than the one in [23], and that it is the tightest possible bound for actual, stationary GMPs when assuming a stationary GMP model.

III. STATIONARY DISCRETE-TIME GMP MODEL

A. Problem Formulation

Discrete-time LDS models are often used in practical applications involving digital computers. They can be described at a time epoch $n \in \mathbb{Z} \geq 0$ using the following equations:

$$\mathbf{x}_n = \mathbf{\Phi}_n \mathbf{x}_{n-1} + \mathbf{w}_n, \tag{22}$$

$$\mathbf{z}_n = \mathbf{H}_n \mathbf{x}_n + \mathbf{v}_n, \tag{23}$$

where $\mathbf{\Phi}$ and $\mathbf{w}$ are the discrete-time transition matrix and process noise vector, respectively. The vector $\mathbf{x}$ is the augmented state vector such that $\mathbf{x}^T = [\boldsymbol{\xi}^T \ \mathbf{a}^T]$ where $\boldsymbol{\xi}$ are the original states of interest and $\mathbf{a}$ are the augmented states. In the same manner as in Section II, GMP models can be incorporated by state augmentation. A discrete-time GMP model can be written as

$$a_n = \hat{\alpha}_\mathrm{d} a_{n-1} + \sqrt{\hat{\sigma}^2_\mathrm{d}\left(1 - \hat{\alpha}^2_\mathrm{d}\right)} w_n, \tag{24}$$

where $\hat{\alpha}_\mathrm{d} = e^{\frac{-\Delta t}{\hat{\tau}_d}}$, $w_n \sim \mathcal{N}(0, 1)$, and $\Delta t \in \mathbb{R}_{>0}$ is the sampling time interval. The quantities $\hat{\tau}_\mathrm{d} \in \mathbb{R}_{>0}$ and $\hat{\sigma}^2_\mathrm{d} \in \mathbb{R}_{\geq 0}$, respectively, are the time constant and variance used in the discrete-time GMP model. We want to find a discrete-time GMP model whose spectral density $\hat{S}_\mathrm{d}$ is greater than or equal to that of the actual GMP S_d, which is expressed as

$$\hat{S}_\mathrm{d}(\omega) \geq S_\mathrm{d}(\omega), \qquad \forall \omega \in \left[0, \frac{\pi}{\Delta t}\right]. \tag{25}$$

Besides, we seek the GMP model that minimizes the total power of the process, i.e., that minimizes $\hat{\sigma}^2_\mathrm{d}$, while satisfying (25).

B. GMP Discrete-Time Model Parameters

THEOREM 2 Let $a_n \in \mathbb{R}$ be a discrete-time, stationary, first-order GMP with uncertain variance $\sigma^2 \in [\sigma^2_{\min}, \sigma^2_{\max}]$ and correlation time constant $\tau \in [\tau_{\min}, \tau_{\max}]$. The variance and correlation time constant of a discrete-time, stationary, first-order GMP model $\hat{a}_n \in \mathbb{R}$ that provides the tightest bound on the PSD of the process a_n can respectively be expressed as

$$\hat{\sigma}^2_\mathrm{d} = \sigma^2_{\max}\sqrt{\frac{(1-\alpha_{\min})(1+\alpha_{\max})}{(1+\alpha_{\min})(1-\alpha_{\max})}}, \quad \text{and} \tag{26}$$

$$\hat{\tau}_\mathrm{d} = -\Delta t \left[\ln\left(\frac{1-\sqrt{\Gamma}}{1+\sqrt{\Gamma}}\right)\right]^{-1}, \tag{27}$$

where

$$\alpha_{\min} = e^{-\frac{\Delta t}{\tau_{\min}}}, \ \alpha_{\max} = e^{-\frac{\Delta t}{\tau_{\max}}}, \ \text{and} \tag{28}$$

$$\Gamma = \frac{(1-\alpha_{\min})(1-\alpha_{\max})}{(1+\alpha_{\min})(1+\alpha_{\max})}. \tag{29}$$

PROOF The spectral density of a generic discrete-time first-order GMP can be expressed as [25]

$$S_\mathrm{d}(\omega) = \frac{\sigma^2 \Delta t \left(1-\alpha^2\right)}{1+\alpha^2 - 2\alpha\cos(\omega\Delta t)}, \tag{30}$$

where $\alpha = e^{\frac{-\Delta t}{\tau}}$. With the definition in (30), the condition in (25) states that for all $\omega \in [0, \frac{\pi}{\Delta t}]$, we must satisfy the inequality

$$\frac{\hat{\sigma}^2_\mathrm{d}\Delta t\left(1-\hat{\alpha}^2_\mathrm{d}\right)}{1+\hat{\alpha}^2_\mathrm{d} - 2\hat{\alpha}_\mathrm{d}\cos(\omega\Delta t)} \geq \frac{\sigma^2\Delta t\left(1-\alpha^2\right)}{1+\alpha^2-2\alpha\cos(\omega\Delta t)}. \tag{31}$$

After bringing the right-hand-side term to the left, expressing the two fractions with a common denominator, and dividing both sides by Δt, (31) becomes

$$\frac{\hat{\sigma}_{\mathrm{d}}^2\left(1-\hat{\alpha}_{\mathrm{d}}^2\right)\left(1+\alpha^2-2\alpha\cos(\omega\Delta t)\right)}{\left(1+\hat{\alpha}_{\mathrm{d}}^2-2\hat{\alpha}_{\mathrm{d}}\cos(\omega\Delta t)\right)\left(1+\alpha^2-2\alpha\cos(\omega\Delta t)\right)} - \frac{\sigma^2\left(1-\alpha^2\right)\left(1+\hat{\alpha}_{\mathrm{d}}^2-2\hat{\alpha}_{\mathrm{d}}\cos(\omega\Delta t)\right)}{\left(1+\hat{\alpha}_{\mathrm{d}}^2-2\hat{\alpha}_{\mathrm{d}}\cos(\omega\Delta t)\right)\left(1+\alpha^2-2\alpha\cos(\omega\Delta t)\right)} \geq 0 \quad \forall\omega \in \left[0, \frac{\pi}{\Delta t}\right]. \tag{32}$$

The second-order polynomials appearing in the denominators are of the form $x^2 - 2x\cos(\omega\Delta t) + 1$. That is, they are parabolas that open up with a minimum value of $1 - \cos^2\omega\Delta t$ occurring at $x^* = \cos\omega\Delta t$. Given that $\cos(\omega\Delta t) \in [-1, 1]$, the minimum value of the parabola is always nonnegative, and since the parabolas open up, it must be that the denominators in (32) are also nonnegative. The case of $\alpha = 1$, which would cause the denominator in (32) to be zero when $\cos^2(\omega\Delta t) = 1$, is not possible since $\Delta t > 0$ and τ is finite. Therefore, (32) is satisfied if and only if (IFF) the numerator is nonnegative, which, after factoring out $\cos(\omega\Delta t)$, can be written as

$$\cos(\omega\Delta t)\left(\sigma^2(1-\alpha^2)2\hat{\alpha}_{\mathrm{d}} - \hat{\sigma}_{\mathrm{d}}^2(1-\hat{\alpha}_{\mathrm{d}}^2)2\alpha\right) + \hat{\sigma}_{\mathrm{d}}^2(1-\hat{\alpha}_{\mathrm{d}}^2)(1+\alpha^2) - \sigma^2(1-\alpha^2)(1+\hat{\alpha}_{\mathrm{d}}^2) \geq 0, \quad \forall\omega \in [0, \frac{\pi}{\Delta t}]. \tag{33}$$

Equation (33) is linear in $\cos(\omega\Delta t)$, which can be written independently of Δt as $\cos(\Omega)$ where $\Omega = \omega\Delta t$, $\forall\Omega \in [0, \pi]$. The term $\cos(\omega\Delta t)$ is a monotonically decreasing function of $\omega\Delta t$ for $\omega \in [0, \pi/\Delta t]$. Thus, showing that the inequality in (33) is satisfied $\forall\omega \in [0, \frac{\pi}{\Delta t}]$ is equivalent to showing that it is satisfied for the limit values of $\cos(\omega\Delta t)$. For $\cos(\omega\Delta t) = 1$, (33) becomes

$$\hat{\sigma}_{\mathrm{d}}^2 \geq \sigma^2\frac{(1+\alpha)(1-\hat{\alpha}_{\mathrm{d}})}{(1-\alpha)(1+\hat{\alpha}_{\mathrm{d}})}. \tag{34}$$

For $\cos(\omega\Delta t) = -1$, (33) becomes

$$\hat{\sigma}_{\mathrm{d}}^2 \geq \sigma^2\frac{(1-\alpha)(1+\hat{\alpha}_{\mathrm{d}})}{(1+\alpha)(1-\hat{\alpha}_{\mathrm{d}})}. \tag{35}$$

Equations (34) and (35) must be satisfied $\forall\sigma^2 \in [\sigma_{\min}^2, \sigma_{\max}^2]$. Choosing $\sigma^2 = \sigma_{\max}^2$ ensures that (34) and (35) are satisfied for any other value of σ^2 within the admissible range. In addition, (34) and (35) must hold for all values of α, i.e., $\forall\,\tau \in [\tau_{\min}, \tau_{\max}]$. In (34), the maximum value of the right-hand-side is for $\alpha = \alpha_{\max}$, which maximizes the numerator while minimizing the denominator because $0 < \alpha < 1$. Similarly, in (35), the maximum value of the right-hand-side is for $\alpha = \alpha_{\min}$. Furthermore, the tightest PSD bound in (25) is found when $\hat{\sigma}_{\mathrm{d}}^2$ is minimized, which is achieved at equality in (34) and (35). We obtain the following two equations:

$$\hat{\sigma}_{\mathrm{d}}^2 = \sigma_{\max}^2\frac{(1+\alpha_{\max})(1-\hat{\alpha}_{\mathrm{d}})}{(1-\alpha_{\max})(1+\hat{\alpha}_{\mathrm{d}})}, \tag{36}$$

$$\hat{\sigma}_{\mathrm{d}}^2 = \sigma_{\max}^2\frac{(1-\alpha_{\min})(1+\hat{\alpha}_{\mathrm{d}})}{(1+\alpha_{\min})(1-\hat{\alpha}_{\mathrm{d}})}. \tag{37}$$

Solving for $\hat{\alpha}_{\mathrm{d}}$ and $\hat{\sigma}_{\mathrm{d}}^2$ in (36) and (37), we find a PSD-bounding, discrete-time, stationary, first-order GMP model with the variance and time constant parameters in (26) and (27). This ends the proof for Theorem 2. ■

COROLLARY 2.1 The estimated covariance matrix of a discrete-time LDS estimator (e.g., a KF) whose measurement and process noise are linear combinations of independent, stationary, first-order GMP with uncertain parameters $\sigma^2 \in [\sigma_{\min}^2, \sigma_{\max}^2]$ and $\tau \in [\tau_{\min}, \tau_{\max}]$ can be tightly bounded in the positive semidefinite sense, in the discrete-time domain, by modeling each independent GMP with a stationary, first-order GMP model with parameters given in (26) and (27).

PROOF Theorem 2 establishes that the PSD of a discrete-time GMP model with parameters in (26) and (27) bounds that of an uncertain GMP with uncertain parameters $\sigma^2 \in [\sigma_{\min}^2, \sigma_{\max}^2]$ and $\tau \in [\tau_{\min}, \tau_{\max}]$. The proof in [23] establishes that bounding the individual PSD of independent and time-correlated process and measurement noises in an LDS provides an estimation error covariance that bounds the true error covariance. Therefore, using a discrete-time GMP model with the parameters in (26) and (27) in an LDS estimator (e.g., a KF) ensures that the modeled estimation error covariance upper bounds the actual estimation error covariance. ■

C. Using Discrete-Time Models With Parameter Values Derived in Continuous-Time

At the limit when Δt tends to 0, the expressions of $\hat{\sigma}_{\mathrm{d}}$ and $\hat{\tau}_{\mathrm{d}}$ in (26) and (27) approach their continuous-time equivalents in (13), i.e.,

$$\lim_{\Delta t\to 0}\hat{\sigma}_{\mathrm{d}} = \hat{\sigma}_{\mathrm{c}}, \tag{38}$$

$$\lim_{\Delta t\to 0}\hat{\tau}_{\mathrm{d}} = \hat{\tau}_{\mathrm{c}}. \tag{39}$$

These equations can be derived, for example, using series expansions of the exponential terms in (26)–(29). Intermediary results to achieve (39) include

$$\lim_{\Delta t\to 0}\sqrt{\Gamma} = \omega_{\mathrm{d}}\Delta t, \tag{40}$$

where $\omega_{\mathrm{d}} = (2\sqrt{\tau_{\min}\tau_{\max}})^{-1}$; the argument of the natural logarithm in (27), therefore, approaches $e^{-2\omega_{\mathrm{d}}\Delta t}$ when $\Delta t \to 0$. The remainder of the derivation is straightforward, and is omitted to limit the length of this article.

The expressions of $\hat{\sigma}_{\mathrm{c}}^2$ and $\hat{\tau}_{\mathrm{c}}$ in (13) for continuous-time GMP models are more compact than their discrete-time equivalents $\hat{\sigma}_{\mathrm{d}}^2$ and $\hat{\tau}_{\mathrm{d}}$ in (26) and (27). There are precedents for using continuous-time parameter values in discrete-time models, e.g., in continuous to discrete-time transformations in [24].

THEOREM 3 Let $a_n \in \mathbb{R}$ be a discrete-time, stationary, first-order GMP model with variance and correlation time constant defined using (26) and (27). The PSD of a discrete-time, stationary, first-order GMP model with variance and correlation time constant defined using (13) upper bounds that of the PSD of a_n regardless of the sampling time interval.

PROOF Theorem 3 can be written in mathematical terms as

$$\frac{\hat{\sigma}_c^2 \Delta t \left(1-\hat{\alpha}_c^2\right)}{1+\hat{\alpha}_c^2-2\hat{\alpha}_c \cos(\omega \Delta t)} \geq \frac{\hat{\sigma}_d^2 \Delta t \left(1-\hat{\alpha}_d^2\right)}{1+\hat{\alpha}_d^2-2\hat{\alpha}_d \cos(\omega \Delta t)}, \quad \forall \Delta t \geq 0 \tag{41}$$

where the left-hand side was obtained by substituting $\hat{\sigma}_c^2$ for σ^2 and $\hat{\tau}_c$ for τ in the definition of $\hat{S}_d(\omega)$ in (30), the right-hand side was obtained by substituting $\hat{\sigma}_d^2$ for σ^2 and $\hat{\tau}_d$ for τ in $\hat{S}_d(\omega)$, and $\hat{\alpha}_c = e^{\frac{-\Delta t}{\hat{\tau}_c}}$.

The inequality in (41) is of the same form as that in (31). Thus, following the same steps as in (31) to (35), we can show that (41) is true IFF the following two inequalities are satisfied for all $\Delta t \geq 0$:

$$\hat{\sigma}_c^2 \frac{(1+\hat{\alpha}_c)}{(1-\hat{\alpha}_c)} \geq \hat{\sigma}_d^2 \frac{(1+\hat{\alpha}_d)}{(1-\hat{\alpha}_d)}, \tag{42}$$

$$\hat{\sigma}_c^2 \frac{(1-\hat{\alpha}_c)}{(1+\hat{\alpha}_c)} \geq \hat{\sigma}_d^2 \frac{(1-\hat{\alpha}_d)}{(1+\hat{\alpha}_d)}. \tag{43}$$

Substituting the expressions of $\hat{\sigma}_d^2$ in (36) and (37) into (42) and (43), respectively, using the definition of $\hat{\sigma}_c^2$ in (13) and dividing both sides by $\sigma_{\max}^2$, the last two inequalities become

$$\sqrt{\frac{\tau_{\max}}{\tau_{\min}}} \frac{(1+\hat{\alpha}_c)}{(1-\hat{\alpha}_c)} \geq \frac{(1+\alpha_{\max})}{(1-\alpha_{\max})}, \tag{44}$$

$$\sqrt{\frac{\tau_{\max}}{\tau_{\min}}} \frac{(1-\hat{\alpha}_c)}{(1+\hat{\alpha}_c)} \geq \frac{(1-\alpha_{\min})}{(1+\alpha_{\min})}. \tag{45}$$

Multiplying both sides of these inequalities by $\sqrt{\tau_{\max}\tau_{\min}} = \hat{\tau}_c$, bringing all terms to the left-hand side, expanding, factoring out $(\tau_{\max} - \hat{\tau}_c)$ and $(\tau_{\max} + \hat{\tau}_c)$, and rearranging, we obtain the following left-hand-side expressions of (44) and (45), respectively:

$$f_1(\Delta t) = (\tau_{\max} - \hat{\tau}_c)(1 - \alpha_{\max}\hat{\alpha}_c) + (\tau_{\max} + \hat{\tau}_c)(\hat{\alpha}_c - \alpha_{\max}), \tag{46}$$

$$f_2(\Delta t) = (\tau_{\max} - \hat{\tau}_c)(1 - \alpha_{\min}\hat{\alpha}_c) + (\tau_{\max} + \hat{\tau}_c)(\alpha_{\min} - \hat{\alpha}_c). \tag{47}$$

Substituting the definitions of $\hat{\alpha}_c$, $\alpha_{\min}$, and $\alpha_{\max}$ into the abovementioned two expressions, the following limits are found:

$$\lim_{\Delta t \to 0} f_1(\Delta t) = 0, \quad \lim_{\Delta t \to 0} f_2(\Delta t) = 0. \tag{48}$$

Thus, we have shown that (41) is satisfied IFF $f_1(\Delta t) \geq 0$ and $f_2(\Delta t) \geq 0, \forall \Delta t \geq 0$. Given (48), this is equivalent to showing that $f_1(\Delta t)$ and $f_2(\Delta t)$ are monotonically increasing, i.e., that their derivatives are nonnegative for all $\Delta t \geq 0$.

First, the derivative of $f_1(\Delta t)$ can be written as

$$f_1'(\Delta t) = \frac{(\tau_{\max} - \hat{\tau}_c)(\tau_{\max} + \hat{\tau}_c)}{\tau_{\max}\hat{\tau}_c} e^{-\frac{\Delta t}{\tau_{\max}}} e^{-\frac{\Delta t}{\hat{\tau}_c}} + \frac{(\tau_{\max} + \hat{\tau}_c)}{\tau_{\max}\hat{\tau}_c} \left(\hat{\tau}_c e^{-\frac{\Delta t}{\tau_{\max}}} - \tau_{\max} e^{-\frac{\Delta t}{\hat{\tau}_c}}\right) \geq 0. \tag{49}$$

Dividing both sides of the inequality by the nonnegative factor $(e^{-\frac{\Delta t}{\tau_{\max}}} e^{-\frac{\Delta t}{\hat{\tau}_c}} \frac{\tau_{\max}+\hat{\tau}_c}{\tau_{\max}\hat{\tau}_c})$ and rearranging, the left-hand side in (49) becomes

$$f_{1,1}(\Delta t) = \hat{\tau}_c \left(e^{\frac{\Delta t}{\hat{\tau}_c}} - 1\right) - \tau_{\max}\left(e^{\frac{\Delta t}{\tau_{\max}}} - 1\right). \tag{50}$$

To show that $f_{1,1}$ is nonnegative, we consider the facts that

$$\lim_{\Delta t \to 0} f_{1,1}(\Delta t) = 0 \tag{51}$$

and that the derivative of $f_{1,1}$ is positive, i.e.,

$$f_{1,1}'(\Delta t) = e^{\frac{\Delta t}{\hat{\tau}_c}} - e^{\frac{\Delta t}{\tau_{\max}}} \geq 0, \quad \forall \Delta t \geq 0 \tag{52}$$

because $\tau_{\max} \geq \hat{\tau}_c$. This proves that $f_1'(\Delta t)$ is nonnegative.

Second, the derivative of $f_2(\Delta t)$ is

$$f_2'(\Delta t) = \frac{(\tau_{\max} - \hat{\tau}_c)(\tau_{\min} + \hat{\tau}_c)}{\tau_{\min}\hat{\tau}_c} e^{-\frac{\Delta t}{\tau_{\min}}} e^{-\frac{\Delta t}{\hat{\tau}_c}} + \frac{(\tau_{\max} + \hat{\tau}_c)}{\tau_{\min}\hat{\tau}_c} \left(\tau_{\min} e^{-\frac{\Delta t}{\hat{\tau}_c}} - \hat{\tau}_c e^{-\frac{\Delta t}{\tau_{\min}}}\right) \geq 0. \tag{53}$$

Dividing both sides of the inequality by the nonnegative factor $(e^{-\frac{\Delta t}{\tau_{\min}}} e^{-\frac{\Delta t}{\hat{\tau}_c}} \frac{1}{\tau_{\max}\hat{\tau}_c})$ and rearranging, the left-hand side in (53) becomes

$$f_{2,1}(\Delta t) = \tau_{\max}\tau_{\min}\left(e^{\frac{\Delta t}{\tau_{\min}}} + 1\right) - \tau_{\max}\hat{\tau}_c\left(e^{\frac{\Delta t}{\hat{\tau}_c}} - 1\right) + \hat{\tau}_c\tau_{\min}\left(e^{\frac{\Delta t}{\tau_{\min}}} - 1\right) - \hat{\tau}_c^2\left(e^{\frac{\Delta t}{\hat{\tau}_c}} + 1\right) \geq 0. \tag{54}$$

To show that $f_{2,1}$ is nonnegative, we consider the facts that

$$\lim_{\Delta t \to 0} f_{2,1}(\Delta t) = 2\tau_{\max}\tau_{\min} - 2\hat{\tau}_c^2 = 0, \tag{55}$$

and that the derivative of $f_{2,1}(\Delta t)$ is

$$f_{2,1}'(\Delta t) = (\tau_{\max} + \hat{\tau}_c)\left(e^{\frac{\Delta t}{\tau_{\min}}} - e^{\frac{\Delta t}{\hat{\tau}_c}}\right) \geq 0, \tag{56}$$

because $\tau_{\min} \leq \hat{\tau}_c$. This proves that $f_2'(\Delta t)$ is nonnegative.

The facts that $f_1'(\Delta t)$ and $f_2'(\Delta t)$ are nonnegative for all $\Delta t \geq 0$ and that the limits of $f_1(\Delta t)$ and $f_2(\Delta t)$ as $\Delta t \to 0$ are nonnegative prove that $f_1(\Delta t) \geq 0$ and $f_2(\Delta t) \geq 0, \forall \Delta t \geq 0$, which ultimately proves Theorem 3. ■

COROLLARY 3.1 The PSD of a discrete-time, stationary, first-order GMP model with variance and correlation time constant defined using (13) upper bounds that of a discrete-time, stationary, first-order GMP with uncertain variance $\sigma^2 \in [\sigma_{\min}^2, \sigma_{\max}^2]$ and correlation time constant $\tau \in [\tau_{\min}, \tau_{\max}]$.

PROOF For clarity and conciseness, we use the notation $S_d(\omega, \sigma^2, \tau)$ rather than $S_d(\omega)$ in (30) to designate the discrete-time PSD of the first-order GMP with variance σ^2 and time constant τ. Theorem 2 shows that $\hat{S}_d(\omega, \hat{\sigma}_d^2, \hat{\tau}_d) \geq S_d(\omega, \sigma^2, \tau)$, $\forall \sigma^2 \in [\sigma_{\min}^2, \sigma_{\max}^2]$, $\forall \tau \in [\tau_{\min}, \tau_{\max}]$. Theorem 3 shows that $\hat{S}_d(\omega, \hat{\sigma}_c^2, \hat{\tau}_c) \geq \hat{S}_d(\omega, \hat{\sigma}_d^2, \hat{\tau}_d)$. Therefore, it must be that $\hat{S}_d(\omega, \hat{\sigma}_c^2, \hat{\tau}_c) \geq S_d(\omega, \sigma^2, \tau)$, $\forall \sigma^2 \in [\sigma_{\min}^2, \sigma_{\max}^2]$, $\forall \tau \in [\tau_{\min}, \tau_{\max}]$. ■

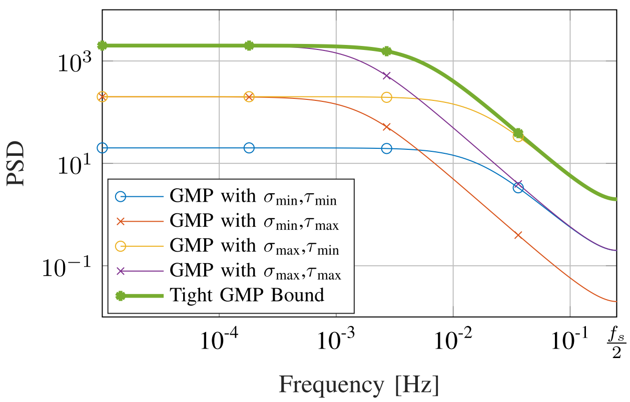

Fig. 2. Discrete-time PSD of stationary GMP with $\sigma^2 \in [1, 10]$ and $\tau \in [10, 100]s$, and new tight bound.

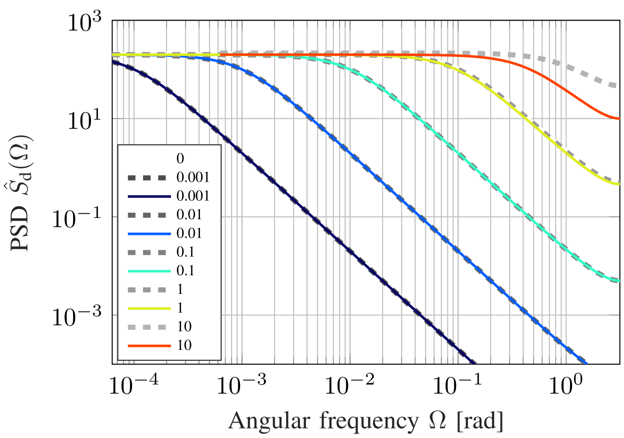

Fig. 3. Discrete-time PSD for first-order GMP models, assuming $\tau \in [1, 100]$ s, $\sigma^2 \in [1, 1]$ (fixed, unitless), for varying values of Δt given in legend (in seconds), using discrete-time parameters (solid) versus continuous-time parameters (dashed).

COROLLARY 3.2 The estimated covariance matrix of a discrete-time LDS estimator (e.g., a KF) whose measurement and process noise are linear combinations of independent, stationary, first-order GMPs with uncertain parameters $\sigma^2 \in [\sigma^2_{\min}, \sigma^2_{\max}]$ and $\tau \in [\tau_{\min}, \tau_{\max}]$ can be upper bounded in the positive semidefinite sense by modeling each independent GMP with a stationary, first-order, discrete-time GMP model with parameters given in (13).

PROOF Corollary 3.1 establishes that the PSD of a discrete-time GMP model with parameters given in (13) upper bounds that of an actual discrete-time GMP with uncertain parameters $\sigma^2 \in [\sigma^2_{\min}, \sigma^2_{\max}]$ and $\tau \in [\tau_{\min}, \tau_{\max}]$. Langel et al. [23] proved that, for linear estimators, the state estimation error covariance matrix is bounded in the positive semidefinite sense if the PSDs of the measurement and process noise models bound those of the actual, independent, time-correlated processes. Therefore, designing a KF using first-order, discrete-time GMP models with parameters given in (13) ensures a bounding state estimation error covariance. ■

Fig. 3 illustrates Theorem 3 for an example discrete-time, first-order GMP described in the figure caption. We assume that $\tau_{\min} = 1$ s, and we consider sampling intervals Δt varying between 0.001 s and 10 s. Using the notations introduced in Corollary 3.1, the solid curves represent $\hat{S}_d(\omega, \hat{\sigma}^2_d, \hat{\tau}_d)$ and the dashed curves are $\hat{S}_d(\omega, \hat{\sigma}^2_c, \hat{\tau}_c)$. For consistency of representation between discrete-time PSDs with varying Δt, the x-axis is displayed in terms of angular frequency $\Omega = 2\pi f \Delta t$, where f is the frequency in Hertz. As demonstrated in Theorem 3, the dashed curves in Fig. 3 upper bound their corresponding solid curves at all frequencies. In addition, it is worth noticing that for values of Δt greater than $\tau_{\min}$, the dashed curves of $\hat{S}_d(\omega, \hat{\sigma}^2_c, \hat{\tau}_c)$ only provide a loose bound on the solid curves representing $\hat{S}_d(\omega, \hat{\sigma}^2_d, \hat{\tau}_d)$. Since Δt and $\tau_{\min}$ are known, a KF designer can make an informed decision on whether to use the GMP parameter expressions in (13) or the ones in (26) and (27) in order to ensure a tightly PSD-bounding model. In many practical problems, Δt is much smaller than $\tau_{\min}$. For example, in [17], the $\tau_{\min}$-values of the time-correlation of satellite orbit and clock errors for GPS and Galileo, respectively, are found to be 4 h and 2 h, while GNSS-based transportation operations require Δt-values lower than 1 s. Therefore, the compact continuous-time GMP parameters in (13) can be both useful and accurate when used in discrete-time models.

IV. NONSTATIONARY CONTINUOUS-TIME GMP MODEL

Theorem 1 and Corollary 1.1 show that an LDS estimator's covariance can be upper bounded by modeling the independent GMP errors as stationary GMPs with parameters defined in (13). However, (13) also shows that the GMP model variance is inflated as compared to the upper bound on the actual process' steady-state variance $\sigma^2_{\max}$: this indicates that the stationary approach is overly-conservative at GMP model initiation. In response, in this section, we derive a nonstationary model that produces the same estimation error covariance bounds at steady state, but tighter bounds during the transient phase. In this sense, the process is nonstationary since its initial variance is different from its steady-state variance and it is changing over time during the transient phase. Appendix D provides more details about the time evolution of the variance for a nonstationary GMP.

THEOREM 4 The estimation error covariance matrix of a continuous-time LDS estimator (e.g., a KF) whose measurement and process noise are linear combinations of independent, stationary, first-order GMPs with uncertain parameters $\sigma^2 \in [\sigma^2_{\min}, \sigma^2_{\max}]$ and $\tau \in [\tau_{\min}, \tau_{\max}]$ can be tightly bounded in a positive semidefinite sense by modeling each independent GMP with a continuous-time, nonstationary, first-order GMP model with steady-state parameters given in (13) and with initial variance defined as

$$\hat{\sigma}^2_{c,0} = \sigma^2_{\max} \frac{2}{1 + \sqrt{\frac{\tau_{\min}}{\tau_{\max}}}}. \quad (57)$$

PROOF In order to show that (57) guarantees a bound on the estimation error covariance, we use the KF sensitivity analysis described in [23]. The prediction step of a KF for the LDS in (1)–(9) can be written as

$$\dot{\hat{\mathbf{x}}} = \hat{\mathbf{F}}\hat{\mathbf{x}}, \tag{58}$$

$$\dot{\hat{\boldsymbol{\Sigma}}}_{\mathbf{x}} = \hat{\mathbf{F}}\hat{\boldsymbol{\Sigma}}_{\mathbf{x}} + \hat{\boldsymbol{\Sigma}}_{\mathbf{x}}\hat{\mathbf{F}}^T + \hat{\mathbf{Q}}, \tag{59}$$

where $\hat{\mathbf{x}}$ is the estimated augmented state vector such that $\hat{\mathbf{x}}^T = [\hat{\boldsymbol{\xi}}^T \; \hat{\mathbf{a}}^T]$. In this proof, we must distinguish true vectors and matrices from the ones assumed by a KF designer. Matrices $\hat{\mathbf{F}}$ and $\hat{\mathbf{Q}}$ are the KF designer's assumed time propagation matrix and process noise covariance matrix, respectively. If $\hat{\mathbf{F}} = \mathbf{F}$ and $\hat{\mathbf{Q}} = \mathbf{Q}$, then the estimated KF state covariance matrix matches the true one, i.e., $\hat{\boldsymbol{\Sigma}}_{\mathbf{x}} = \mathbf{P}_{\mathbf{x}}$. If $\hat{\mathbf{F}}$ and $\hat{\mathbf{Q}}$ are not the true matrices, the propagation of true errors can be expressed using the following differential equation [23]:

$$\begin{bmatrix} \dot{\mathbf{e}} \\ \dot{\mathbf{a}} \end{bmatrix} = \begin{bmatrix} \hat{\mathbf{F}} & \Delta\mathbf{F} \\ \mathbf{0} & \mathbf{L} \end{bmatrix} \begin{bmatrix} \mathbf{e} \\ \mathbf{a} \end{bmatrix} + \begin{bmatrix} -\mathbf{w} \\ \mathbf{u} \end{bmatrix}, \tag{60}$$

where the true error is defined as $\mathbf{e} \triangleq \hat{\mathbf{x}} - \mathbf{x}$ and $\Delta\mathbf{F} \triangleq \hat{\mathbf{F}} - \mathbf{F}$. The difference $\Delta\mathbf{F}$ between designed and true $\mathbf{F}$ is caused by the unknown correlation time constant $\tau \in [\tau_{\min}, \tau_{\max}]$ in (7). Therefore, we can write $\Delta\mathbf{F} \triangleq [\mathbf{0}^T \, \Delta\mathbf{L}^T]^T$ where $\Delta\mathbf{L} \triangleq \hat{\mathbf{L}} - \mathbf{L}$. Matrices $\hat{\mathbf{L}}$ and $\mathbf{L}$, respectively, are the designed and true matrices of the GMP time propagation model in (7). The KF true error covariance matrix associated with (60) is

$$\dot{\mathbf{P}} = \begin{bmatrix} \hat{\mathbf{F}} & \Delta\mathbf{F} \\ \mathbf{0} & \mathbf{L} \end{bmatrix} \mathbf{P} + \mathbf{P} \begin{bmatrix} \hat{\mathbf{F}} & \Delta\mathbf{F} \\ \mathbf{0} & \mathbf{L} \end{bmatrix}^T + \mathbf{Q}. \tag{61}$$

To be able to compare (61) with the error covariance of the designed KF, we can extend (59) as

$$\dot{\boldsymbol{\Sigma}} = \begin{bmatrix} \hat{\mathbf{F}} & \mathbf{0} \\ \mathbf{0} & \mathbf{L} \end{bmatrix} \boldsymbol{\Sigma} + \boldsymbol{\Sigma} \begin{bmatrix} \hat{\mathbf{F}} & \mathbf{0} \\ \mathbf{0} & \mathbf{L} \end{bmatrix}^T + \begin{bmatrix} \hat{\mathbf{Q}} & \mathbf{0} \\ \mathbf{0} & \bar{\mathbf{Q}} \end{bmatrix}, \tag{62}$$

where $\boldsymbol{\Sigma}$ is a block diagonal matrix including the designed KF covariance matrix in the upper left block

$$\dot{\boldsymbol{\Sigma}} = \begin{bmatrix} \dot{\hat{\boldsymbol{\Sigma}}}_{\mathbf{x}} & \mathbf{0} \\ \mathbf{0} & \dot{\bar{\boldsymbol{\Sigma}}}_{\mathbf{a}} \end{bmatrix}, \tag{63}$$

where $\dot{\bar{\boldsymbol{\Sigma}}}_{\mathbf{a}}$ is the covariance matrix of the augmented states and $\dot{\boldsymbol{\Sigma}}$ is of the same dimensions as $\dot{\mathbf{P}}$ in (61). The assumed error covariance matrix bounds the true error's in a positive semidefinite sense IFF $\boldsymbol{\Sigma} - \mathbf{P} \geq 0$, which is equivalent to guaranteeing the following two inequalities [23]:

$$\dot{\boldsymbol{\Sigma}} - \dot{\mathbf{P}} \geq 0, \;\; \boldsymbol{\Sigma}(0) - \mathbf{P}(0) \geq 0. \tag{64}$$

We can derive tight GMP bounds using nonstationary GMP models with initial variance lower than that of the stationary model, but still satisfying the second inequality in (64). Using the expression of $\boldsymbol{\Sigma}$ derived in [23], this second inequality is satisfied IFF

$$\begin{bmatrix} \boldsymbol{\Sigma}_{\xi}(0) - \mathbf{P}_{\xi}(0) & \mathbf{0} & \mathbf{0} \\ \mathbf{0} & \hat{\boldsymbol{\Sigma}}_{\mathrm{a}}(0) - \mathbf{P}_{\mathrm{a}}(0) & \mathbf{P}_{\mathrm{a}}(0) \\ \mathbf{0} & \mathbf{P}_{\mathrm{a}}(0) & \bar{\boldsymbol{\Sigma}}_{\mathrm{a}}(0) - \mathbf{P}_{\mathrm{a}}(0) \end{bmatrix} \geq \mathbf{0} \tag{65}$$

where $\hat{\boldsymbol{\Sigma}}_{\mathrm{a}}(0)$ is the designed KF's initial GMP covariance matrix and $\bar{\boldsymbol{\Sigma}}_{\mathrm{a}}(0) = \bar{\boldsymbol{\Sigma}}_{\mathrm{a}}$ is the covariance of the stationary GMPs propagated in the lower right block of $\boldsymbol{\Sigma}$ in (62). Both $\hat{\boldsymbol{\Sigma}}_{\mathrm{a}}(0)$ and $\bar{\boldsymbol{\Sigma}}_{\mathrm{a}}$ are determined below to ensure that (64) is satisfied. It is worth noticing that $\mathbf{P}_{\mathrm{a}}(0) = \mathbf{P}_{\mathrm{a}}$ since the true GMP processes are assumed to be stationary. Without loss of generality on the impact of uncertain time correlation, we can assume that the KF designer's unaugmented state covariance initialization ensures that $\boldsymbol{\Sigma}_{\xi}(0) - \mathbf{P}_{\xi}(0) \geq 0$. Therefore, the need to satisfy (65) reduces to showing that the following inequality holds:

$$\begin{bmatrix} \hat{\boldsymbol{\Sigma}}_{\mathrm{a}}(0) - \mathbf{P}_{\mathrm{a}} & \mathbf{P}_{\mathrm{a}} \\ \mathbf{P}_{\mathrm{a}} & \bar{\boldsymbol{\Sigma}}_{\mathrm{a}}(0) - \mathbf{P}_{\mathrm{a}} \end{bmatrix} \geq \mathbf{0}. \tag{66}$$

All four matrix blocks in (66) are diagonal since they capture the initial variance of independent GMP processes. Therefore, for a 2×2 block corresponding to a single independent process, (66) can be rewritten as

$$\begin{bmatrix} \hat{\sigma}^2_{\mathrm{c},0} - \sigma^2 & \sigma^2 \\ \sigma^2 & \bar{\sigma}^2_{\mathrm{c}} - \sigma^2 \end{bmatrix} \geq \mathbf{0}, \tag{67}$$

which imposes the following lower bound on $\hat{\sigma}^2_{\mathrm{c},0}$

$$\hat{\sigma}^2_{\mathrm{c},0} \geq \sigma^2 + \frac{\sigma^4}{\bar{\sigma}^2_{\mathrm{c}} - \sigma^2}. \tag{68}$$

Equation (68) must be valid for any value of the unknown parameters σ^2 and τ. This is ensured, first, by choosing $\sigma^2 = \sigma^2_{\max}$. Then, $\bar{\sigma}^2_{\mathrm{c}}$ depends on σ^2 and τ: we can find the minimum value of $\bar{\sigma}^2_{\mathrm{c}}$ ensuring that (68) is satisfied for any values of σ^2 and τ. In Appendix A, an expression of $\bar{\sigma}^2_{\mathrm{c,min}}$ is derived from the first inequality in (64). Appendix A shows that, for the bounds in (13), $\bar{\sigma}^2_{\min}$ can be expressed as

$$\bar{\sigma}^2_{\mathrm{c,min}} = 2\sigma^2_{\max} \frac{\tau_{\max}}{\tau_{\max} - \hat{\tau}}. \tag{69}$$

Substituting (69) into (68), we obtain

$$\hat{\sigma}^2_{\mathrm{c},0} \geq \sigma^2_{\max} + \frac{\sigma^4_{\max}(\tau_{\max} - \hat{\tau})}{2\sigma^2_{\max}\tau_{\max} - \sigma^2_{\max}(\tau_{\max} - \hat{\tau})}. \tag{70}$$

Using $\hat{\tau} = \sqrt{\tau_{\min}\tau_{\max}}$ from (13) and rearranging, the tightest bound on $\hat{\sigma}^2_{\mathrm{c},0}$ is found at equality, which is (57). ■

V. NONSTATIONARY DISCRETE-TIME GMP MODEL

A. Analytical Solution

THEOREM 5 The estimation error covariance matrix of a discrete-time LDS estimator (e.g., a KF) whose measurement and process noise are linear combinations of independent, stationary, first-order GMPs with uncertain parameters $\sigma^2 \in [\sigma^2_{\min}, \sigma^2_{\max}]$ and $\tau \in [\tau_{\min}, \tau_{\max}]$ can be tightly bounded in a positive semidefinite sense by modeling each independent GMP with a discrete-time, nonstationary, first-order GMP model with steady-state parameters given in (26) and (27) and with initial variance defined as

$$\hat{\sigma}^2_{\mathrm{d},0} = \sigma^2_{\max} \frac{1}{1 - \dfrac{2(\hat{\alpha}_{\mathrm{d}} - \alpha_{\max})^2}{(1 - \hat{\alpha}^2_{\mathrm{d}})(1 - \alpha^2_{\max})(k_{\mathrm{d}} - 1)}} \tag{71}$$

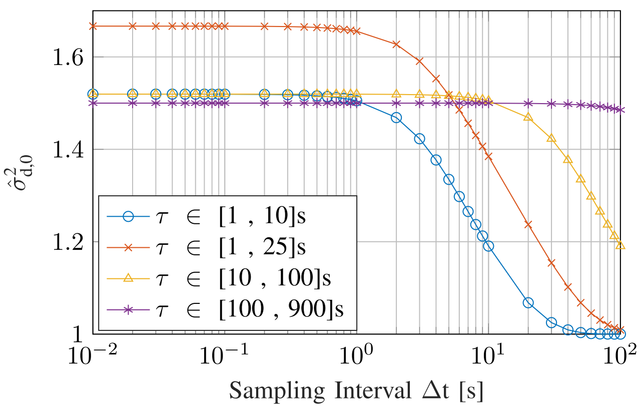

Fig. 4. Initial variance of nonstationary GMP bounding model for different τ-ranges and $\sigma^2_{\max} = 1$.

where

$$k_{\mathrm{d}} = \sqrt{\frac{(1-\alpha_{\min})(1+\alpha_{\max})}{(1+\alpha_{\min})(1-\alpha_{\max})}}. \tag{72}$$

PROOF We follow an approach similar to that in the continuous-time case in Section IV. In [23], the authors showed that the discrete-time KF estimation error variance could be bounded if the following inequalities were satisfied:

$$\begin{aligned} \mathbf{\Sigma}_{k|k-1} - \mathbf{P}_{k|k-1} &\geq \mathbf{0}, \quad \forall k \in [1, \infty) \\ \mathbf{\Sigma}_0 - \mathbf{P}_0 &\geq \mathbf{0}. \end{aligned} \tag{73}$$

The conditions in (73) are the discrete-time versions of (64). And they are also introduced in Appendix B. While still satisfying bounding conditions at steady state, it is possible to design a KF filter incorporating nonstationary GMPs to provide a tighter estimation error bound during the initial transient phase. The initialization state estimation error bound is imposed by the second condition in (73), which can be written similar to (65) as

$$\begin{bmatrix} \mathbf{\Sigma}_{\xi,0} - \mathbf{P}_{\xi,0} & \mathbf{0} & \mathbf{0} \\ \mathbf{0} & \hat{\mathbf{\Sigma}}_{\mathrm{a},0} - \mathbf{P}_{\mathrm{a},0} & \mathbf{P}_{\mathrm{a},0} \\ \mathbf{0} & \mathbf{P}_{\mathrm{a},0} & \bar{\mathbf{\Sigma}}_{\mathrm{a},0} - \mathbf{P}_{\mathrm{a},0} \end{bmatrix} \geq \mathbf{0} \tag{74}$$

Following the same reasoning as in Section IV, for each GMP under consideration, (74) reduces to

$$\hat{\sigma}^2_{\mathrm{d},0} \geq \sigma^2 + \frac{\sigma^4}{\bar{\sigma}^2_{\mathrm{d}} - \sigma^2}. \tag{75}$$

Appendix B shows that, for the GMP parameters in (26) and (27), the minimum stationary variance $\bar{\sigma}^2_{\mathrm{d}}$ that guarantees (75) for the range of possible values of $\bar{\sigma}^2_{\mathrm{d}}$, and therefore, σ^2 and τ can be expressed in the discrete-time case as

$$\bar{\sigma}^2_{\mathrm{d,min}} = \frac{(1-\hat{\alpha}^2_{\mathrm{d}})(1-\alpha^2_{\max})}{2(\hat{\alpha}_{\mathrm{d}}-\alpha_{\max})^2}\left(\hat{\sigma}^2_{\mathrm{d}} - \sigma^2_{\max}\right). \tag{76}$$

Using (26) and (27) and substituting (76) into (75) leads to (71), where $\sigma^2 = \sigma^2_{\max}$ has been chosen to guarantee (75) for any possible value of σ^2. ■

Fig. 4 shows values of $\hat{\sigma}^2_{\mathrm{d},0}$ for example ranges of τ-values over sampling time intervals Δt ranging from 0.01 s to 100 s. When $\Delta t \ll \tau$ the minimum initial variance converges to a single value. In the case that the time interval approaches the value of the time-correlation constant, it is possible to reduce the minimum initial variance. This is due to the whitening effect of lower sampling frequencies on the processes.

B. Discrete Nonstationary Model Using Parameters Derived in Continuous-Time

THEOREM 6 The estimation error covariance matrix of a discrete-time LDS estimator (e.g., a KF) whose measurement and process noise are linear combinations of independent, stationary, first-order GMPs with uncertain parameters $\sigma^2 \in [\sigma^2_{\min}, \sigma^2_{\max}]$ and $\tau \in [\tau_{\min}, \tau_{\max}]$ can be tightly bounded in a positive semidefinite sense by modeling each independent GMP with a discrete-time, nonstationary, first-order GMP model with steady-state parameters given in (13) and with initial variance values defined in (57).

PROOF Theorem 3 establishes that, at steady state, the GMP parameter values derived in the continuous-time domain can be used in discrete-time models to provide an error-variance-bounded KF solution. This implies that using (13) in discrete-time models satisfies the first condition in (73). Theorem 6 extends the use of parameter values derived in the continuous-time domain to nonstationary discrete-time GMP models. The proof reduces to showing that the second condition in (73) holds when the initial variance value in (57) is used. This is equivalent to showing that $\hat{\sigma}^2_{\mathrm{c},0}$ in (57) is larger than or equal to $\hat{\sigma}^2_{\mathrm{d},0}$ when the parameter values derived in the continuous-time domain [see (13)] are used, i.e.,

$$\hat{\sigma}^2_{\mathrm{c},0} \geq \hat{\sigma}^2_{\mathrm{d},0}(\hat{\sigma}^2_{\mathrm{c}}, \hat{\tau}_{\mathrm{c}}), \quad \forall \Delta t > 0. \tag{77}$$

Comparing the expressions of $\hat{\sigma}^2_{\mathrm{c},0}$ and $\hat{\sigma}^2_{\mathrm{d},0}$ in (68) and (75), (77) holds IFF the minimum values of $\bar{\sigma}^2$ satisfy

$$\bar{\sigma}^2_{\mathrm{c,min}} \leq \bar{\sigma}^2_{\mathrm{d,min}}(\hat{\sigma}^2_{\mathrm{c}}, \hat{\tau}_{\mathrm{c}}) \quad \forall \Delta t > 0. \tag{78}$$

Proof of (78) is given in Appendix C. It ensures that (77) holds and, therefore, proves Theorem 6. ■

C. Numerical Solution for Finite Filter Duration

Section V provides an expression for the initial variance of a nonstationary discrete-time GMP bounding process. This GMP model ensures an upper bound on the KF variance regardless of the filtering duration, including for infinite horizons. In some applications, time-correlated measurements can only be used over a finite duration; for example, a GPS satellite is visible for no longer than 12 h at a time at a static ground receiver location. In this section, we provide an alternative approach to compute the initial variance of a discrete-time nonstationary GMP model whose use is expected to be limited in time. The new numerically computed initial variance provides an even tighter nonstationary GMP bound than in Section V. This new model still matches the stationary GMP at steady state, but provides a tighter estimation error variance bound during the transient period.

We start by deriving, in Appendix D, the autocovariance r_{np} of a nonstationary discrete-time GMP between any two time steps n and p where $n \in \mathbb{Z} \geq 0$, $p \in \mathbb{Z} \geq 0$, and $p \geq n$. r_{np}. As a function of the initial variance σ_0^2, r_{np} can be expressed as

$$r_{\text{np}} = E\left[a_n a_p^T\right] = \hat{\alpha}^{n+p}\sigma_0^2 + \hat{\sigma}^2(1-\hat{\alpha}^{2n})\hat{\alpha}^{p-n}, \tag{79}$$

where $\hat{\alpha} = e^{\frac{-\Delta t}{\tau}}$, $a_0 \sim \mathcal{N}(0, \sigma_0^2)$, and $w_n \sim \mathcal{N}(0, 1)$. Without loss of generality the values of $\hat{\alpha}$ and $\hat{\sigma}^2$ can be either the ones derived in the continuous or in the discrete-time domain as summarized in Table I.

We use a numerical approach to find the minimum value of σ_0^2 that guarantees an upper bound on the estimation error variance. σ_0^2 only needs to be determined once for each noise component, i.e., for each range of $\sigma^2 \in [\sigma_{\min}^2, \sigma_{\max}^2]$ and $\tau \in [\tau_{\min}, \tau_{\max}]$. This process can be performed offline prior to KF initialization and does not cause extra computational load when running the KF.

The autocovariance matrix (ACM) of size N (maximum epoch duration of the time-correlated process in the filter) of the bounding nonstationary GMP model is

$$\hat{\mathbf{R}}(N) = \begin{bmatrix} r_{00} & r_{01} & \cdots & r_{0\,N} \\ r_{01} & r_{11} & \cdots & r_{1\,N} \\ \vdots & \vdots & \ddots & \vdots \\ r_{0\,N} & r_{1\,N} & \cdots & r_{NN} \end{bmatrix}. \tag{80}$$

The actual, unknown stationary GMP ACM is expressed as

$$\mathbf{R}(N) = \begin{bmatrix} \sigma^2 & \alpha\sigma^2 & \cdots & \alpha^N\sigma^2 \\ \alpha\sigma^2 & \sigma^2 & \cdots & \alpha^{N-1}\sigma^2 \\ \vdots & \vdots & \ddots & \vdots \\ \alpha^N\sigma^2 & \alpha^{N-1}\sigma^2 & \cdots & \sigma^2 \end{bmatrix}. \tag{81}$$

Equation (81) is obtained by setting $\sigma_0^2 = \sigma^2$ and by replacing $\hat{\sigma}^2 = \sigma^2$ and $\hat{\alpha}$ with $\alpha = e^{\frac{-\Delta t}{\tau}}$ in (79), and substituting the result into (80).

In [15], the authors show that overbounding the KF estimation error in the presence of time-correlated process and measurement errors can be achieved by finding an ACM $\hat{\mathbf{R}}$ such that the difference between $\hat{\mathbf{R}}$ and $\mathbf{R}$ is positive semidefinite. Therefore it must be ensured that

$$\Delta\mathbf{R} = \hat{\mathbf{R}} - \mathbf{R} = \hat{\mathbf{R}} - \sigma^2\bar{\mathbf{R}} \geq \mathbf{0}, \tag{82}$$

where σ^2 has been factored out from $\mathbf{R}$ in (81) and $\bar{\mathbf{R}}$ is the autocorrelation matrix. Matrix $\Delta\mathbf{R}$ in (82) must be positive semidefinite for all values of $\sigma^2 \in [\sigma_{\min}^2, \sigma_{\max}^2]$ and $\tau \in [\tau_{\min}, \tau_{\max}]$. If $\Delta\mathbf{R}$ is positive semidefinite for $\sigma^2 = \sigma_{\max}^2$, then it is positive semidefinite for all possible values of σ^2.

Using $\sigma^2 = \sigma_{\max}^2$ and the notation $\hat{\sigma}^2 = \sigma_{\max}^2 k$, where k is either the multiplier in (13) or the one in (26), and introducing the notation $\sigma_0^2 = \sigma_{\max}^2 k_0$, (82) can be expressed over a finite number of time epochs N as

$$\Delta\mathbf{R}(N, k_0) = \sigma_{\max}^2 \begin{bmatrix} k_0 - 1 & \cdots & \hat{\alpha}^{n-1}k_0 - \alpha^{N-1} \\ \vdots & \ddots & \vdots \\ \cdots & \cdots & \hat{\alpha}^{2N}k_0 + k\left(1 - \hat{\alpha}^{2N}\right) - 1 \end{bmatrix}. \tag{83}$$

The minimum acceptable value of k_0 is the smallest one guaranteeing that $\Delta\mathbf{R}$ is positive semidefinite [23]. In order to find k_0, we use the fact that the eigenvalues of a real symmetric matrix are real, and that the matrix is positive semidefinite IFF its minimum eigenvalue is nonnegative. For the symmetric matrix $\Delta\mathbf{R}(N)$ with minimum eigenvalue $\lambda_{\min}$, we must ensure that $\lambda_{\min}(N) \geq 0, \forall N \in \mathbb{Z}_{\geq 0}$. The numerical search for σ_0^2 can be expressed as

$$\sigma_0^2 = \sigma_{\max}^2 \cdot \arg\min_{k_x} \{\lambda_{\min}(\Delta\mathbf{R}(N, k_x)) \geq 0\}. \tag{84}$$

A good initialization point for the numerical search is provided in Appendix E. It ensures that the first 2×2 leading principal minor of $\Delta\mathbf{R}$ is positive semidefinite.

VI. SUMMARY OF THE KF DESIGN

Let us consider a discrete-time state-augmented LDS model expressed as

$$\begin{bmatrix} \boldsymbol{\xi}_n \\ \mathbf{a}_n \end{bmatrix} = \begin{bmatrix} \boldsymbol{\Phi}_n & \mathbf{E}_{\text{w}} \\ \mathbf{0} & \mathbf{L}_n \end{bmatrix} \begin{bmatrix} \boldsymbol{\xi}_{n-1} \\ \mathbf{a}_{n-1} \end{bmatrix} + \begin{bmatrix} \boldsymbol{\eta}_n \\ \mathbf{u}_n \end{bmatrix},$$
$$\mathbf{z}_n = \begin{bmatrix} \mathbf{H}_n & \mathbf{E}_{\text{v}} \end{bmatrix} \begin{bmatrix} \boldsymbol{\xi}_n \\ \mathbf{a}_n \end{bmatrix} + \boldsymbol{\nu}_n, \tag{85}$$

and let us make the following definitions:

$$\mathbf{x}_n = \begin{bmatrix} \boldsymbol{\xi}_n \\ \mathbf{a}_n \end{bmatrix}, \ \mathbf{A}_n = \begin{bmatrix} \boldsymbol{\Phi}_n & \mathbf{E}_{\text{w}} \\ \mathbf{0} & \mathbf{L}_n \end{bmatrix}, \ \mathbf{C}_n = \begin{bmatrix} \mathbf{H}_n & \mathbf{E}_{\text{v}} \end{bmatrix},$$
$$\mathbf{Q}_n = E\left[\begin{bmatrix} \boldsymbol{\eta}_n \\ \mathbf{u}_n \end{bmatrix} \begin{bmatrix} \boldsymbol{\eta}_n^T & \mathbf{u}_n^T \end{bmatrix}\right] = \begin{bmatrix} \mathbf{N}_n & \mathbf{0} \\ \mathbf{0} & \mathbf{U}_n \end{bmatrix}. \tag{86}$$

GMP matrices $\mathbf{L}$ and $\mathbf{U}$, and hence, $\mathbf{A}$ and $\mathbf{Q}$, are uncertain. In previous sections, we derived expressions for the parameters in $\hat{\mathbf{L}}$ and $\hat{\mathbf{U}}$ that account for that uncertainty. The KF can therefore be written as

$$\mathbf{x}_{n|n-1} = \hat{\mathbf{A}}_n \mathbf{x}_{n-1|n-1}, \tag{87}$$
$$\hat{\mathbf{P}}_{n|n-1} = \hat{\mathbf{A}}_n \hat{\mathbf{P}}_{n-1|n-1} \hat{\mathbf{A}}_n^T + \hat{\mathbf{Q}}_n, \tag{88}$$
$$\hat{\mathbf{K}}_n = \hat{\mathbf{P}}_{n|n-1} \hat{\mathbf{C}}_n^T \left(\hat{\mathbf{C}}_n \hat{\mathbf{P}}_{n|n-1} \hat{\mathbf{C}}_n^T + \mathbf{R}_n\right)^{-1}, \tag{89}$$
$$\mathbf{x}_{n|n} = \mathbf{x}_{n|n-1} + \hat{\mathbf{K}}_n \left(\mathbf{z}_n - \hat{\mathbf{C}}_n \mathbf{x}_{n|n-1}\right), \tag{90}$$
$$\hat{\mathbf{P}}_{n|n} = \left(\mathbf{I} - \hat{\mathbf{K}}_n \hat{\mathbf{C}}_n\right) \hat{\mathbf{P}}_{n|n-1}. \tag{91}$$

In the case where $\hat{\mathbf{A}} = \mathbf{A}$ and $\hat{\mathbf{Q}} = \mathbf{Q}$, the KF state covariance matrix coincides with the true error covariance, i.e., $\hat{\mathbf{P}} = \mathbf{P}$. We designed $\hat{\mathbf{L}}$ and $\hat{\mathbf{U}}$, and hence, $\hat{\mathbf{A}}$ and $\hat{\mathbf{Q}}$, such that $\hat{\mathbf{P}} \geq \mathbf{P}$. We then tightened the bound on $\mathbf{P}$ considering a nonstationary GMP model implemented using the initial KF covariance matrix $\hat{\mathbf{P}}_0$. Matrices $\hat{\mathbf{L}}$, $\hat{\mathbf{U}}$, and $\hat{\mathbf{P}}_0$ can be

TABLE I
Summary of GMP Bounding Model Parameters

	Continuous-time domain* (for $\tau_{\max} \geq \tau_{\min} > 0$)	Discrete-time domain (for $\tau_{\max} \geq \tau_{\min} \geq 0$)
Stationary model	$\hat{\tau}_{\mathrm{c}} = \sqrt{\tau_{\min}\tau_{\max}}$, $\hat{\sigma}_{\mathrm{c}}^2 = \sqrt{\frac{\tau_{\max}}{\tau_{\min}}}\sigma_{\max}^2$.	$\hat{\sigma}_{\mathrm{d}}^2 = \sigma_{\max}^2 \sqrt{\frac{(1-\alpha_{\min})(1+\alpha_{\max})}{(1+\alpha_{\min})(1-\alpha_{\max})}}$, $\hat{\tau}_{\mathrm{d}} = -\Delta t \left[\ln\left(\frac{1-\sqrt{\Gamma}}{1+\sqrt{\Gamma}}\right)\right]^{-1}$, where $\alpha_{\min} = e^{-\frac{\Delta t}{\tau_{\min}}}$, $\alpha_{\max} = e^{-\frac{\Delta t}{\tau_{\max}}}$, $\Gamma = \frac{(1-\alpha_{\min})(1-\alpha_{\max})}{(1+\alpha_{\min})(1+\alpha_{\max})}$.
Non-stationary model (initial variance)	$\hat{\sigma}_{\mathrm{c},0}^2 = \sigma_{\max}^2 \frac{2}{1+\sqrt{\frac{\tau_{\min}}{\tau_{\max}}}}$.	$\hat{\sigma}_{\mathrm{d},0} = \sigma_{\max}^2 \frac{1}{1-\frac{2(\hat{\alpha}-\alpha_{\max})^2}{(1-\hat{\alpha}^2)(1-\alpha_{\max}^2)(k_{\mathrm{d}}-1)}}$, where $k_{\mathrm{d}} = \sqrt{\frac{(1-\alpha_{\min})(1+\alpha_{\max})}{(1+\alpha_{\min})(1-\alpha_{\max})}}$.

*Continuous-time model parameter values can also be used in discrete-time models (see Section III-C and Section V-B).

expressed as

$$\hat{\mathbf{L}} = \mathrm{diag}\left[e^{-\Delta t/\hat{\tau}_1}, \ldots, e^{-\Delta t/\hat{\tau}_l}\right], \tag{92}$$

$$\hat{\mathbf{U}} = \mathrm{diag}\left[\hat{\sigma}_1^2\left(1-e^{-\frac{2\Delta t}{\hat{\tau}_1}}\right), \ldots, \hat{\sigma}_l^2\left(1-e^{-\frac{2\Delta t}{\hat{\tau}_l}}\right)\right], \tag{93}$$

$$\hat{\mathbf{P}}_0 = \begin{bmatrix}\mathbf{P}_{\boldsymbol{\xi},0} & \\ & \hat{\mathbf{P}}_{\mathbf{a},0}\end{bmatrix}, \tag{94}$$

with

$$\hat{\mathbf{P}}_{\mathbf{a},0} = \mathrm{diag}\left[\hat{\sigma}_{0,1}^2, \ldots, \hat{\sigma}_{0,l}^2\right], \tag{95}$$

where for independent GMPs $i = 1, \ldots, l$, $\hat{\tau}_i$, $\hat{\sigma}_i^2$, and $\hat{\sigma}_{0,i}^2$ can be computed using the expressions in Table I.

VII. EXAMPLE KF IMPLEMENTATION

In order to evaluate the new GMP models, we consider the motivational example described in [23], where the initial position and constant velocity of a vehicle moving along a one-dimensional trajectory is estimated using time-correlated ranging signals. The LDS includes an augmented state to account for measurement error time-correlation. The LDS is described by the following equations:

$$\begin{bmatrix} p_{0,n} \\ v_n \\ a_n \end{bmatrix} = \begin{bmatrix} 1 & 0 & 0 \\ 0 & 1 & 0 \\ 0 & 0 & \alpha \end{bmatrix}\begin{bmatrix} p_{0,n-1} \\ v_{n-1} \\ a_{n-1} \end{bmatrix} + \begin{bmatrix} 0 \\ 0 \\ \sqrt{q_d}w_n \end{bmatrix}, \tag{96}$$

$$z_n = \begin{bmatrix} 1 & n\Delta t & 1 \end{bmatrix}\begin{bmatrix} p_{0,n} \\ v_n \\ a_n \end{bmatrix} + \nu_n, \tag{97}$$

with

$$\begin{aligned}\alpha &= e^{\frac{-\Delta t}{\tau}}, \\ q_d &= \sigma_a^2(1-e^{\frac{-2\Delta t}{\tau}}),\end{aligned} \quad \text{and} \quad \begin{aligned} w_n &= \mathcal{N}(0,1), \\ \nu_n &= \mathcal{N}\left(0, \sigma_\nu^2\right),\end{aligned} \tag{98}$$

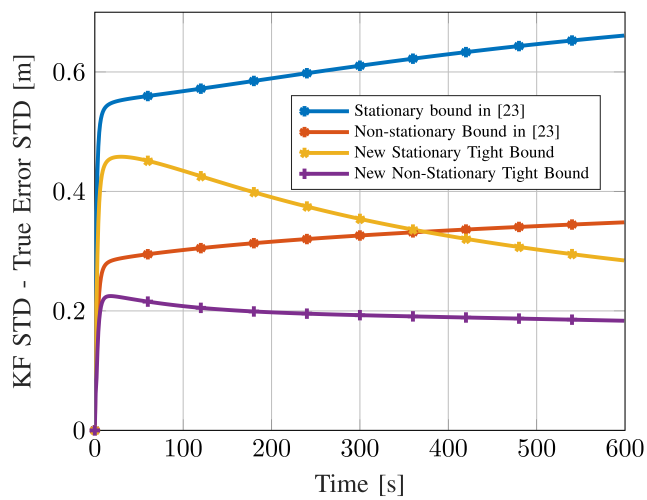

Fig. 5. KF estimated error versus true error (position) ($\tau_{\max} = 100$, $\tau_{\min} = 10$, $\tau_{\mathrm{true}} = 50$, and $\Delta t = 1$ s).

where p_0, v are the initial position and speed of the vehicle and a is the augmented state. z is the ranging measurement.

τ is only known to be in the range $\tau \in [10, 100]$s, $\sigma_\nu^2 = 1$, and $\sigma_{\mathrm{a}}^2 = 1$. The initial estimate error covariance matrix $\mathbf{P}_0$ is diagonal with nonzero elements of 10 m^2 for the position state, 1 $\mathrm{m}^2/\mathrm{s}^2$ for the speed state. The initial variance for the augmented state depends on the model under evaluation.

Fig. 5 shows the difference between the standard deviation of the position estimated using a KF and that of the true estimation error. For computation of the true estimated error of a discrete-time KF, the reader may consult [22, Appendix B]. Fig. 5 displays the stationary and nonstationary GMP models derived in [23] and those derived in Sections III and

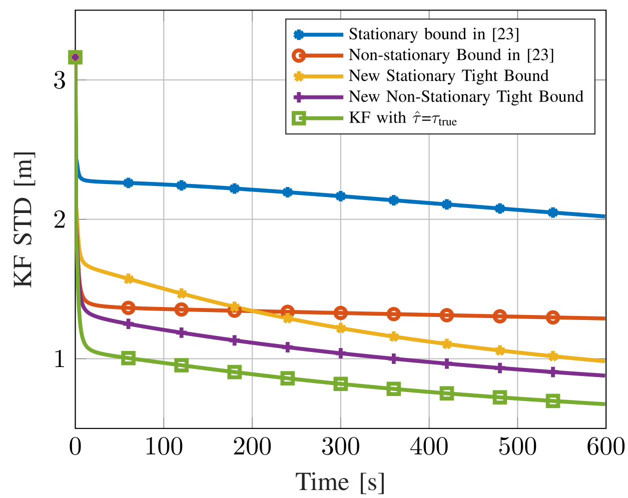

Fig. 6. KF standard deviation (Position) ($\tau_{\max} = 100$, $\tau_{\min} = 10$, $\tau_{\text{true}} = 50$, and $\Delta t = 1$s).

V of this article. Positive values of the curves mean that the GMP models all produce upper bounds on the positioning variance. If the simulation time was long enough, we would see positioning deviations using the nonstationary GMP models converge towards their corresponding stationary GMP models.

We focus on the transient period. We can see that over the first 300 s of simulation time, the nonstationary GMP model in [23] provides a tighter positioning deviation bound than the stationary model in this article. But, as filtering approaches steady-state, our proposed stationary model in Section III provides a tighter bound on the true error standard deviation. The nonstationary GMP model in Section V achieves the tightest positioning error bound.

In addition, Fig. 6 shows the KF positioning standard deviations for the new GMP models as compared to those in [23], and to the KF standard deviation obtained if we knew the true value of correlation time constant. This figure illustrates the inflation in standard deviation that we endure for lack of knowledge of the actual error correlation time constant, and the tightness of the positioning variance bounds obtained using the proposed GMP models.

VIII. CONCLUSION

In this article, we derived the stationary GMP model that guarantees the tightest upper bound on linear estimation error variance in the presence of uncertain time-correlated measurement and process errors with first-order Gauss–Markov structure. We analyzed the PSD of GMPs to obtain stationary models in both continuous-time and discrete-time domains. The stationary models were improved upon using continuous-time and discrete-time nonstationary GMP models, which provide tighter estimation error variance bound during the transient period. These GMP models can easily be implemented in linear dynamic estimators such as KFs. We used an example positioning application to illustrate the fact that the proposed estimation error bounds can be significantly tighter than those described in prior publications.

APPENDIX A
DERIVATION OF $\bar{\Sigma}$ IN CONTINUOUS-TIME DOMAIN

This Appendix aims at deriving an expression for the diagonal elements of matrix $\bar{\Sigma}_{\text{a}}$ in (65). The derivation evaluates the first inequality in (64) using the continuous-time stationary bounds in (13). The first condition in (64) is

$$\dot{\mathbf{\Sigma}} - \dot{\mathbf{P}} \geq \mathbf{0}. \tag{99}$$

Because (62) does not have the same propagation matrices as (61), we first rewrite (62) as

$$\dot{\mathbf{\Sigma}} = \begin{bmatrix} \hat{\mathbf{F}} & \Delta\mathbf{F} \\ \mathbf{0} & \mathbf{L} \end{bmatrix} \mathbf{\Sigma} + \mathbf{\Sigma} \begin{bmatrix} \hat{\mathbf{F}} & \Delta\mathbf{F} \\ \mathbf{0} & \mathbf{L} \end{bmatrix}^T + \begin{bmatrix} \hat{\mathbf{Q}} & -\Delta\mathbf{F}\mathbf{\Sigma}_{\text{a}} \\ -\mathbf{\Sigma}_{\text{a}}\Delta\mathbf{F}^T & \bar{\mathbf{Q}} \end{bmatrix}. \tag{100}$$

Substituting (61) and (100) into (99) and using the notation $\mathbf{\Delta} = \mathbf{\Sigma} - \mathbf{P}$ leads to

$$\dot{\mathbf{\Delta}} = \begin{bmatrix} \hat{\mathbf{F}} & \Delta\mathbf{F} \\ \mathbf{0} & \mathbf{L} \end{bmatrix} \mathbf{\Delta} + \mathbf{\Delta} \begin{bmatrix} \hat{\mathbf{F}} & \Delta\mathbf{F} \\ \mathbf{0} & \mathbf{L} \end{bmatrix}^T + \begin{bmatrix} \hat{\mathbf{Q}}_\xi - \mathbf{Q}_\xi & \mathbf{0} & \mathbf{0} \\ \mathbf{0} & \hat{\mathbf{Q}}_{\text{a}} - \mathbf{Q}_{\text{a}} & -\Delta\mathbf{L}\mathbf{\Sigma}_{\text{a}} + \mathbf{Q}_{\text{a}} \\ \mathbf{0} & -\mathbf{\Sigma}_{\text{a}}\Delta\mathbf{L}^T + \mathbf{Q}_{\text{a}} & \bar{\mathbf{Q}}_{\text{a}} - \mathbf{Q}_{\text{a}} \end{bmatrix}. \tag{101}$$

Equation (99) is satisfied if $\mathbf{\Delta}(0) \geq \mathbf{0}$ and if the last matrix in (101) is positive semidefinite. The process noise of the unaugmentated states can be chosen by the KF designer to ensure $\hat{\mathbf{Q}}_\xi - \mathbf{Q}_\xi \geq \mathbf{0}$. Therefore ensuring the matrix expression in (101) is positive semidefinite narrows down to showing that

$$\begin{bmatrix} \hat{\mathbf{Q}}_{\text{a}} - \mathbf{Q}_{\text{a}} & -\Delta\mathbf{L}\mathbf{\Sigma}_{\text{a}} + \mathbf{Q}_{\text{a}} \\ -\mathbf{\Sigma}_{\text{a}}\Delta\mathbf{L}^T + \mathbf{Q}_{\text{a}} & \bar{\mathbf{Q}}_{\text{a}} - \mathbf{Q}_{\text{a}} \end{bmatrix} \geq \mathbf{0}. \tag{102}$$

Because we are assuming that the individual noise processes are mutually uncorrelated, the four blocks in (102) are diagonal and the condition in (102) for each noise component can be written as

$$\begin{bmatrix} \hat{q} - q & -\delta l\bar{\sigma}^2 + q \\ -\delta l\bar{\sigma}^2 + q & \bar{q} - q \end{bmatrix} \geq \mathbf{0}, \tag{103}$$

where

$$\delta l = \frac{1}{\tau} - \frac{1}{\hat{\tau}},\ q = \frac{2\sigma^2}{\tau},\ \hat{q} = \frac{2\hat{\sigma}^2}{\hat{\tau}},\ \text{and},\ \bar{q} = \frac{2\bar{\sigma}^2}{\tau}. \tag{104}$$

Using Schur complements to force the off-diagonal terms to be zero, (103) becomes

$$\begin{bmatrix} \hat{q} - q - (q - \delta l\bar{\sigma}^2)^2(\bar{q} - q)^{-1} & 0 \\ 0 & \bar{q} - q \end{bmatrix} \geq \mathbf{0}. \tag{105}$$

Since (105) is diagonal, it will be positive semidefinite if the diagonal elements are nonnegative. Using (104), the first diagonal element can be expressed as

$$\hat{q} - q - \left(q + \frac{\tau}{2}\left(\frac{1}{\hat{\tau}} - \frac{1}{\tau}\right)\bar{q}\right)^2 (\bar{q} - q)^{-1} \geq 0. \quad (106)$$

Multiplying both sides of the inequality by the positive quantity $(\bar{q} - q)$ leads to

$$\hat{q}\bar{q} - \hat{q}q - \bar{q}q - \tau\left(\frac{1}{\hat{\tau}} - \frac{1}{\tau}\right)q\bar{q} - \frac{\tau^2}{4}\left(\frac{1}{\hat{\tau}} - \frac{1}{\tau}\right)^2 \bar{q}^2 \geq 0. \quad (107)$$

Grouping terms in $\bar{q}$, we can write the following quadratic equation:

$$-\frac{\tau^2}{4}\left(\frac{1}{\hat{\tau}} - \frac{1}{\tau}\right)^2 \bar{q}^2 + \left(\hat{q} - \frac{\tau}{\hat{\tau}}q\right)\bar{q} - \hat{q}q \geq 0. \quad (108)$$

Using (104), the previous inequality becomes

$$-\left(\frac{1}{\hat{\tau}} - \frac{1}{\tau}\right)^2 \bar{\sigma}^4 + \frac{\left(\hat{\sigma}^2 - \sigma^2\right)}{\hat{\tau}}\frac{4}{\tau}\bar{\sigma}^2 - \frac{4\hat{\sigma}^2\sigma^2}{\hat{\tau}\tau} \geq 0, \quad (109)$$

which represents the positive values of a parabola of the form $y(x) = ax^2 + bx + c$ where $x = \bar{\sigma}^2$. For given values of σ^2 and τ, there is a range of solutions for $\bar{\sigma}^2$. However, we must find a value of $\bar{\sigma}^2$ that is *always* a solution, for any value of σ^2 and τ within the admissible range. We use the parameters in (13) for $\hat{\sigma}^2$ and $\hat{\tau}$, and we known that $\hat{\sigma}^2 \geq \sigma^2, \forall\sigma^2 \in [\sigma^2_{\min}, \sigma^2_{\max}]$.

Both the quadratic polynomial parameters b and c in the inequality of (109) reduce with increasing values of σ^2. This results in the parabola shifting down and hence reducing the range of possible solutions for $\bar{\sigma}^2$. Therefore, carrying out the derivation for $\sigma^2 = \sigma^2_{\max}$ ensures the most restrictive solution interval for $\bar{\sigma}^2$, which then guarantees a possible solution for other values of σ^2. In addition, with respect to τ, the most restrictive range of $\bar{\sigma}^2$-solutions is found when there is a single possible solution. This solution can be found by ensuring that the polynomial in (109) has a single, repeated root. For $\sigma^2 = \sigma^2_{\max}$, (109) has the following solutions at equality:

$$\bar{\sigma}^2 = \frac{-\frac{4\left(\hat{\sigma}^2 - \sigma^2_{\max}\right)}{\hat{\tau}\tau} \pm \sqrt{\left(\frac{4\left(\hat{\sigma}^2 - \sigma^2_{\max}\right)}{\hat{\tau}\tau}\right)^2 - 16\left(\frac{1}{\hat{\tau}} - \frac{1}{\tau}\right)^2 \frac{\hat{\sigma}^2\sigma^2_{\max}}{\hat{\tau}\tau}}}{-2\left(\frac{1}{\hat{\tau}} - \frac{1}{\tau}\right)^2} \quad (110)$$

which simplifies to

$$\bar{\sigma}^2 = 2\hat{\tau}\tau\frac{\hat{\sigma}^2 - \sigma^2_{\max} \pm \sqrt{\hat{\sigma}^4 + \sigma^4_{\max} - \hat{\sigma}^2\sigma^2_{\max}\frac{\tau^2 + \hat{\tau}^2}{\hat{\tau}\tau}}}{(\tau - \hat{\tau})^2}. \quad (111)$$

Equation (111) has a single value when the argument under the square root is zero. This happens whether we choose $\tau = \tau_{\min}$ or $\tau = \tau_{\max}$. We find the following expression for $\bar{\sigma}^2$:

$$\bar{\sigma}^2_{\min} = 2\sigma^2_{\max}\frac{(\tau_{\max} - \hat{\tau})\,\tau}{(\hat{\tau} - \tau)^2}, \quad \forall\tau = \{\tau_{\min}, \tau_{\max}\}. \quad (112)$$

For instance for $\tau = \tau_{\max}$, (112) becomes

$$\bar{\sigma}^2_{\min} = 2\sigma^2_{\max}\frac{\tau_{\max}}{\tau_{\max} - \hat{\tau}}. \quad (113)$$

APPENDIX B
DERIVATION OF $\bar{\mathbf{\Sigma}}$ IN DISCRETE-TIME DOMAIN

A discrete-time LDS error-state space realization capturing the uncertainty in time-correlated GMP models by state augmentation can be expressed as [23]

$$\begin{bmatrix}\mathbf{e}_k\\ \mathbf{a}_k\end{bmatrix} = \begin{bmatrix}\hat{\mathbf{F}} & \Delta\mathbf{F}\\ \mathbf{0} & \mathbf{L}\end{bmatrix}\begin{bmatrix}\mathbf{e}_{k-1}\\ \mathbf{a}_{k-1}\end{bmatrix} + \begin{bmatrix}-\mathbf{w}_k\\ \mathbf{u}_k\end{bmatrix}. \quad (114)$$

The associated predicted covariance matrix is given by

$$\mathbf{P}_{k|k-1} = \begin{bmatrix}\hat{\mathbf{F}} & \Delta\mathbf{F}\\ \mathbf{0} & \mathbf{L}\end{bmatrix}\mathbf{P}_{k-1|k-1}\begin{bmatrix}\hat{\mathbf{F}} & \Delta\mathbf{F}\\ \mathbf{0} & \mathbf{L}\end{bmatrix}^T + \mathbf{Q}_k. \quad (115)$$

The state-augmented KF covariance matrix can be written as

$$\mathbf{\Sigma}_{k|k-1} = \begin{bmatrix}\hat{\mathbf{F}} & \mathbf{0}\\ \mathbf{0} & \mathbf{L}\end{bmatrix}\mathbf{\Sigma}_{k-1|k-1}\begin{bmatrix}\hat{\mathbf{F}} & \mathbf{0}\\ \mathbf{0} & \mathbf{L}\end{bmatrix}^T + \begin{bmatrix}\hat{\mathbf{Q}}_k & \mathbf{0}\\ \mathbf{0} & \bar{\mathbf{Q}}_k\end{bmatrix}, \quad (116)$$

where $\mathbf{\Sigma}$ is a block diagonal matrix. In order to compare (115) and (116), we introduce off-diagonal matrix blocks in (116) and rewrite the covariance matrix propagation equation as

$$\mathbf{\Sigma}_{k|k-1} = \begin{bmatrix}\hat{\mathbf{F}} & \Delta\mathbf{F}\\ \mathbf{0} & \mathbf{L}\end{bmatrix}\mathbf{\Sigma}_{k-1|k-1}\begin{bmatrix}\hat{\mathbf{F}} & \Delta\mathbf{F}\\ \mathbf{0} & \mathbf{L}\end{bmatrix}^T + \begin{bmatrix}\hat{\mathbf{Q}}_k - \Delta\mathbf{F}\mathbf{\Sigma}_a\Delta\mathbf{F}^T & -\Delta\mathbf{F}\mathbf{\Sigma}_a\mathbf{L}^T\\ -\mathbf{L}\mathbf{\Sigma}_a\Delta\mathbf{F}^T & \bar{\mathbf{Q}}_k\end{bmatrix}. \quad (117)$$

An expression for $\bar{\mathbf{Q}}_k$ can be obtained by considering the first condition in (73). Using the notation $\mathbf{\Delta} = \mathbf{\Sigma} - \mathbf{P}$, the difference between (115) and (117) is

$$\mathbf{\Delta}_{k|k-1} = \begin{bmatrix}\hat{\mathbf{F}} & \Delta\mathbf{F}\\ \mathbf{0} & \mathbf{L}\end{bmatrix}\mathbf{\Delta}_{k-1|k-1}\begin{bmatrix}\hat{\mathbf{F}} & \Delta\mathbf{F}\\ \mathbf{0} & \mathbf{L}\end{bmatrix}^T + \begin{bmatrix}\hat{\mathbf{Q}}_{\xi,k} - \mathbf{Q}_{\xi,k} & \mathbf{0} & \mathbf{0}\\ \mathbf{0} & \hat{\mathbf{Q}}_a - \Delta\mathbf{L}\mathbf{\Sigma}_a\Delta\mathbf{L}^T - \mathbf{Q}_a & -\Delta\mathbf{L}\mathbf{\Sigma}_a\mathbf{L}^T + \mathbf{Q}_a\\ \mathbf{0} & -\mathbf{L}\mathbf{\Sigma}_a\Delta\mathbf{L}^T + \mathbf{Q}_a & \bar{\mathbf{Q}}_k - \mathbf{Q}_a\end{bmatrix} \quad (118)$$

where $\Delta\mathbf{L} \triangleq \hat{\mathbf{L}} - \mathbf{L}$. Since $\mathbf{\Delta}_0 \geq \mathbf{0}$ (as ensured in Section V), $\mathbf{\Delta}_{k|k-1} \geq \mathbf{0}, \forall k \geq 1$ if the last matrix in (118) is positive semidefinite. For the states of interest ξ, we can assume that the process noise covariance matrix is designed such that $\hat{\mathbf{Q}}_{\xi,k} - \mathbf{Q}_{\xi,k} \geq \mathbf{0}$. Therefore, the desired condition $(\mathbf{\Delta}_{k|k-1} \geq \mathbf{0}, \forall k \geq 1)$ is satisfied if the matrix component made of the 2×2 lower right blocks of the rightmost matrix in (118) is positive semidefinite. Since the measurement error GMPs are assumed to be mutually independent, this is equivalent to satisfying the following inequality for each independent GMP:

$$\begin{bmatrix}\hat{q} - (\hat{\alpha} - \alpha)^2\bar{\sigma}^2 - q & -(\hat{\alpha} - \alpha)\alpha\bar{\sigma}^2 + q\\ -(\hat{\alpha} - \alpha)\alpha\bar{\sigma}^2 + q & \bar{q} - q\end{bmatrix} \geq 0, \quad (119)$$

where $\bar{q} = \bar{\sigma}^2(1-\alpha^2)$, $q = \sigma^2(1-\alpha^2)$ and $\hat{q} = \hat{\sigma}^2(1-\hat{\alpha}^2)$. This inequality is satisfied if the matrix determinant is nonnegative, which can be written as

$$\begin{aligned} &-(\alpha-\hat{\alpha})^2\bar{\sigma}^4 + (1-\alpha^2)(1-\hat{\alpha}^2)(\hat{\sigma}^2-\sigma^2)\bar{\sigma}^2 \\ &-\hat{\sigma}^2\sigma^2(1-\alpha^2)(1-\hat{\alpha}^2) \geq 0. \end{aligned} \tag{120}$$

Similar to the continuous-time case in Appendix A, we can solve this quadratic polynomial in $\bar{\sigma}^2$. The smallest $\bar{\sigma}^2$ satisfying (120) for the stationary model parameters in (26) and (27), and valid for all σs and τs, is the value achieved when assuming $\sigma^2 = \sigma^2_{\max}$ and either $\alpha = \alpha_{\min}$ or $\alpha = \alpha_{\max}$. For $\alpha = \alpha_{\max}$, the minimum solution of $\bar{\sigma}^2$ is

$$\bar{\sigma}^2_{\mathrm{d,min}} = \frac{(1-\hat{\alpha}_{\mathrm{d}}^2)(1-\alpha^2_{\max})}{2(\hat{\alpha}_{\mathrm{d}}-\alpha_{\max})^2}\left(\hat{\sigma}^2_{\mathrm{d}} - \sigma^2_{\max}\right). \tag{121}$$

APPENDIX C
PROOF OF THEOREM 6

This appendix aims at proving (78), which can be rewritten as

$$\bar{\sigma}^2_{\mathrm{d,min}}(\hat{\sigma}^2_{\mathrm{c}}, \hat{\tau}_{\mathrm{c}}) - \bar{\sigma}^2_{\mathrm{c,min}} \geq 0, \quad \forall \Delta t > 0. \tag{122}$$

Appendix A gives the following expression of $\bar{\sigma}^2_{\mathrm{c,min}}$:

$$\bar{\sigma}^2_{\mathrm{c,min}} = 2\sigma^2_{\max}\frac{\tau_{\max}}{\tau_{\max}-\hat{\tau}_{\mathrm{c}}}. \tag{123}$$

In order to obtain $\bar{\sigma}^2_{\mathrm{d,min}}(\hat{\sigma}^2_{\mathrm{c}}, \hat{\tau}_{\mathrm{c}})$, we consider the quadratic condition on $\bar{\sigma}^2$ in (120). Similar to Appendix A, we are interested in finding the maximum of the quadratic function in (120), which is

$$\begin{aligned} \bar{\sigma}^2 = &\frac{(1-\alpha)(1-\hat{\alpha}^2)(\hat{\sigma}^2-\sigma^2)}{2(\alpha-\hat{\alpha})^2} \\ &+ \frac{\left\{(1-\alpha^2)(1-\hat{\alpha}^2)^2(\hat{\sigma}^2-\sigma^2)^2 - \right.}{2(\alpha-\hat{\alpha})^2} \\ &\frac{\left. 4(\alpha-\hat{\alpha})^2\hat{\sigma}^2\sigma^2(1-\alpha^2)(1-\hat{\alpha}^2)\right\}^{1/2}}{2(\alpha-\hat{\alpha})^2}. \end{aligned} \tag{124}$$

In the case where $\hat{\alpha} = \hat{\alpha}_{\mathrm{c}}$ (i.e., $\hat{\tau} = \hat{\tau}_{\mathrm{c}}$) and $\hat{\sigma}^2 = \hat{\sigma}^2_{\mathrm{c}}$, the term under the square root in (124) is not zero in general, but it must be a positive value, which we note $\varepsilon \geq 0$. $\bar{\sigma}^2_{\mathrm{d}}(\hat{\sigma}^2_{\mathrm{c}}, \hat{\tau}_{\mathrm{c}})$ can then be written as

$$\bar{\sigma}^2_{\mathrm{d}}\left(\hat{\sigma}^2_{\mathrm{c}}, \hat{\tau}_{\mathrm{c}}\right) = \frac{(1-\alpha)\left(1-\hat{\alpha}^2_{\mathrm{c}}\right)\left(\hat{\sigma}^2_{\mathrm{c}}-\sigma^2\right)}{2(\alpha-\hat{\alpha}_{\mathrm{c}})^2} + \varepsilon. \tag{125}$$

This expression can be minimized while accounting for all possible values of σ and τ when setting $\sigma^2 = \sigma^2_{\max}$, and when either $\alpha = \alpha_{\min}$ or $\alpha = \alpha_{\max}$. Substituting (125) and (123) into (122), it becomes

$$\frac{(1-\alpha)(1-\hat{\alpha}^2_{\mathrm{c}})(\hat{\sigma}^2_{\mathrm{c}}-\sigma^2_{\max})}{2(\alpha-\hat{\alpha}_{\mathrm{c}})^2} + \varepsilon - 2\sigma^2_{\max}\frac{\tau_{\max}}{\tau_{\max}-\hat{\tau}} \geq 0. \tag{126}$$

Substituting $\hat{\sigma}^2_{\mathrm{c}}$ in (13) into (126), factoring $\sigma^2_{\max}$ out, and rearranging the two fractions, we obtain the following inequality:

$$\begin{aligned} \sigma^2_{\max}\Bigg[&\frac{(\tau_{\max}-\hat{\tau}_{\mathrm{c}})(1-\alpha)(1-\hat{\alpha}^2_{\mathrm{c}})\left(\sqrt{\frac{\tau_{\max}}{\tau_{\min}}}-1\right)}{2\left(\alpha-\hat{\alpha}_{\mathrm{c}}\right)^2\left(\tau_{\max}-\hat{\tau}_{\mathrm{c}}\right)} \\ &-\frac{4\tau_{\max}(\alpha-\hat{\alpha}_{\mathrm{c}})^2}{2(\alpha-\hat{\alpha}_{\mathrm{c}})^2(\tau_{\max}-\hat{\tau}_{\mathrm{c}})}\Bigg] + \varepsilon \geq 0. \end{aligned} \tag{127}$$

Since $\tau_{\max} \geq \hat{\tau}_{\mathrm{c}}$, the denominator is larger than zero and the condition in (127) reduces to ensuring that the numerator is larger than or equal to zero. This is the case because: (a) at the limit, the numerator approaches zero when $\Delta t \to 0$ and (b) the numerator is a monotonically increasing function of Δt independent of the actual value of τ. We can prove this by taking the derivative of the numerator, which is given by

$$\begin{aligned} &(\tau_{\max}-\hat{\tau}_{\mathrm{c}})(k_{\mathrm{c}}-1)\left[\frac{2(1-e^{\frac{-\Delta t}{\tau}})e^{\frac{-2\Delta t}{\hat{\tau}_{\mathrm{c}}}}}{\hat{\tau}_{\mathrm{c}}} + \frac{e^{\frac{-\Delta t}{\tau}}(1-e^{\frac{-2\Delta t}{\hat{\tau}_{\mathrm{c}}}})}{\tau}\right] \\ &-8\tau_{\max}\left(e^{\frac{-\Delta t}{\tau}} - e^{\frac{-\Delta t}{\hat{\tau}_{\mathrm{c}}}}\right)\left(\frac{e^{\frac{-\Delta t}{\hat{\tau}_{\mathrm{c}}}}}{\hat{\tau}_{\mathrm{c}}} - \frac{e^{\frac{-\Delta t}{\tau}}}{\tau}\right) \geq 0. \end{aligned} \tag{128}$$

Since $k_{\mathrm{c}} = \sqrt{\frac{\tau_{\max}}{\tau_{\min}}} \geq 1$, and since the exponentials with negative exponents have values ranging between 0 and 1, the first term in (128) is always positive. The second term with a (-8) multiplier can be rewritten as

$$-8\frac{\tau_{\max}}{\hat{\tau}_{\mathrm{c}}\tau}\left(e^{\frac{-\Delta t}{\tau}} - e^{\frac{-\Delta t}{\hat{\tau}_{\mathrm{c}}}}\right)e^{\frac{-\Delta t}{\hat{\tau}_{\mathrm{c}}}}e^{\frac{-\Delta t}{\tau}}\left(\tau e^{\frac{\Delta t}{\tau}} - \hat{\tau}_{\mathrm{c}}e^{\frac{-\Delta t}{\hat{\tau}_{\mathrm{c}}}}\right) \geq 0. \tag{129}$$

If $\tau < \hat{\tau}_{\mathrm{c}}$, $(e^{\frac{-\Delta t}{\tau}} - e^{\frac{-\Delta t}{\hat{\tau}_{\mathrm{c}}}}) < 0$ and $(\tau e^{\frac{\Delta t}{\tau}} - \hat{\tau}_{\mathrm{c}}e^{\frac{-\Delta t}{\hat{\tau}_{\mathrm{c}}}}) > 0$, then (129) is positive. If $\tau > \hat{\tau}_{\mathrm{c}}$, $(e^{\frac{-\Delta t}{\tau}} - e^{\frac{-\Delta t}{\hat{\tau}_{\mathrm{c}}}}) > 0$ and $(\tau e^{\frac{\Delta t}{\tau}} - \hat{\tau}_{\mathrm{c}}e^{\frac{-\Delta t}{\hat{\tau}_{\mathrm{c}}}}) < 0$, then (129) is also positive. In the case where $\tau = \hat{\tau}_{\mathrm{c}}$, (129) is zero. This proves that (128) is nonnegative, ultimately proving (122).

APPENDIX D
NONSTATIONARY GMP COVARIANCE OVER TIME

This Appendix provides an expression for the autocovariance of a general nonstationary discrete-time GMP between two time steps. The first three samples of the discrete-time GMP sequence can be expressed with respect to the initial GMP sample a_0 as

$$\begin{aligned} a_1 &= \alpha a_0 + \sqrt{\sigma^2(1-\alpha^2)}w_1, \\ a_2 &= \alpha^2 a_0 + \alpha\sqrt{\sigma^2(1-\alpha^2)}w_1 + \sqrt{\sigma^2(1-\alpha^2)}w_2, \\ a_3 &= \alpha^3 a_0 + \alpha^2\sqrt{\sigma^2(1-\alpha^2)}w_1 + \alpha\sqrt{\sigma^2(1-\alpha^2)}w_2 \\ &\quad + \sqrt{\sigma^2(1-\alpha^2)}w_3, \\ &\;\;\vdots \end{aligned} \tag{130}$$

where

$$\alpha = e^{\frac{-\Delta t}{\tau}}, \quad \text{and } w_i \sim \mathcal{N}(0,1), \quad \forall i \in \mathbb{Z} > 0. \tag{131}$$

A general, compact form of these equations can be written for any time step n as

$$a_n = \alpha^n a_0 + \sqrt{\sigma^2(1-\alpha^2)} \sum_{i=0}^{n-1} \alpha^i w_{n-i}. \tag{132}$$

Since the expected value of a GMP is zero for any time step ($E[a_n] = 0,\ \forall n \geq 0$), the autocovariance of this nonstationary process between any two time steps $n \in \mathbb{Z}$ and $p \in \mathbb{Z}$ with $p \geq n$ is

$$\begin{aligned} E[a_n a_p] &= E\left[\left(\alpha^n a_0 + \sqrt{\sigma^2(1-\alpha^2)} \sum_{i=0}^{n-1} \alpha^i w_{n-i}\right)\right. \\ &\quad \left.\times \left(\alpha^p a_0 + \sqrt{\sigma^2(1-\alpha^2)} \sum_{j=0}^{p-1} \alpha^j w_{p-j}\right)\right]. \end{aligned} \tag{133}$$

Using the notation $E[a_0^2] = \sigma_0^2$, the fact that $E[a_0 w_i] = 0,\ \forall i \in \mathbb{Z} > 0$, and rearranging, (133) becomes

$$\begin{aligned} E[a_n a_p] &= \alpha^n \alpha^p \sigma_0^2 \\ &\quad + \sigma^2(1-\alpha^2) \sum_{i=0}^{n-1} \sum_{j=0}^{p-1} \alpha^i \alpha^j E[w_{n-i} w_{p-j}]. \end{aligned} \tag{134}$$

Because the driving noise w_i is a white sequence, the expectation function under the double summation in (134) is nonzero only if $n - i = p - j$, which is expressed as

$$\begin{aligned} E[w_i w_i] &= 1, \quad \forall i > 0, \\ E[w_i w_j] &= 0, \ \text{for } i \neq j. \end{aligned} \tag{135}$$

Therefore, we can make the change of variable: $j = p - n + i$ to get rid of one of the two summations

$$E[a_n a_p] = \alpha^n \alpha^p \sigma_0^2 + \sigma^2(1-\alpha^2) \sum_{i=0}^{n-1} \alpha^{2i+p-n}. \tag{136}$$

Recognizing a geometric series, (136) becomes

$$E[a_n a_p] = \alpha^n \alpha^p \sigma_0^2 + \sigma^2(1-\alpha^2) \frac{(\alpha^{2n}-1)\alpha^{p-n}}{\alpha^2 - 1} \tag{137}$$

which finally leads to

$$E[a_n a_p] = \alpha^{n+p} \sigma_0^2 + \sigma^2(1-\alpha^{2n})\alpha^{p-n}, \qquad \forall p \geq n. \tag{138}$$

It is worth noting that if the process is stationary (i.e., $\sigma_0^2 = \sigma^2$), then (138) expectedly reduces to

$$E[a_n a_p] = \sigma^2 \alpha^{p-n}, \qquad \forall p \geq n. \tag{139}$$

The correlation between two time steps is the same regardless of the order of indices, that is: $E[a_n a_p] = E[a_p a_n]$. With this in mind, we can give an expression that does not specify which of n or p is larger

$$E[a_n a_p] = \alpha^{n+p} \sigma_0^2 + \sigma^2(1-\alpha^{2\min(n,p)})\alpha^{|p-n|}. \tag{140}$$

APPENDIX E
APPROXIMATE NONSTATIONARY INITIAL VARIANCE INFLATION FACTOR

In order to support the numerical search of k_0, we can use the fact that the impact of k_0 on the positive semidefiniteness of $\Delta\mathbf{R}$ is most significant on the first leading principal minors. A first good approximation of $\tilde{k}_0$ can, therefore, be obtained by considering the first 2×2 leading principal submatrix. This is obtained by considering $N = 2$, $n = 0$, and $p = 1$ in (83), which reduces to

$$\sigma_{\max}^2 \begin{bmatrix} k_0 - 1 & \hat{\alpha} k_0 - \alpha \\ \hat{\alpha} k_0 - \alpha & \hat{\alpha}^2 k_0 + k\left(1 - \hat{\alpha}^2\right) - 1 \end{bmatrix} \succeq 0. \tag{141}$$

This inequality leads to the following condition on $\tilde{k}_0$:

$$\tilde{k}_0 \geq \frac{k\left(1-\hat{\alpha}^2\right) - 1 + \alpha^2}{k\left(1-\hat{\alpha}^2\right) - 1 - \hat{\alpha}^2 + 2\alpha\hat{\alpha}}. \tag{142}$$

The right-hand side of (142) is larger when $\tau = \tau_{\min}$. Therefore, the most restrictive condition on $\tilde{k}_0$ is

$$\tilde{k}_0 \geq \frac{k\left(1 - e^{-\frac{2\Delta t}{\hat{\tau}}}\right) - 1 + e^{-\frac{2\Delta t}{\tau_{\min}}}}{k\left(1 - e^{-\frac{2\Delta t}{\hat{\tau}}}\right) - 1 - e^{-\frac{2\Delta t}{\hat{\tau}}} + 2e^{-\Delta t\left(\frac{1}{\hat{\tau}} + \frac{1}{\tau_{\min}}\right)}}. \tag{143}$$

The value in (143) has been observed to be very close to the minimum condition on k_0. It is a good initialization value for the search of k_0. It is noteworthy in this discrete time expression that the minimum value of k_0 depends on the values and range of τ and on the sample interval Δt. The impact of Δt becomes significant when Δt approaches $\tau_{\min}$.

REFERENCES

[1] J. Lee, S. Pullen, and P. Enge, "Sigma overbounding using a position domain method for the local area augmentaion of GPS," *IEEE Trans. Aerosp. Electron. Syst.*, vol. 45, no. 4, pp. 1262–1274, Oct. 2009.

[2] J. Rife and B. Pervan, "Overbounding revisited: Discrete error-distribution modeling for safety-critical GPS navigation," *IEEE Trans. Aerosp. Electron. Syst.*, vol. 48, no. 2, pp. 1537–1551, Apr. 2012.

[3] B. Decleene, "Defining pseudorange integrity—overbounding," in *Proc. Inst. Navigat. ION-GPS*, Jun. 2000, pp. 1916–1924.

[4] J. Rife, S. Pullen, P. Enge, and B. Pervan, "Paired overbounding for nonideal LAAS and WAAS error distributions," *IEEE Trans. Aerosp. Electron. Syst.*, vol. 42, no. 4, pp. 1386–1395, Oct. 2006.

[5] J. Blanch, T. Walter, and P. Enge, "Gaussian bounds of sample distributions for integrity analysis," *IEEE Trans. Aerosp. Electron. Syst.*, vol. 55, no. 4, pp. 1806–1815, Aug. 2019.

[6] L. Xie, Y. C. Soh, and C. E. de Souza, "Robust Kalman filtering for uncertain discrete-time systems," *IEEE Trans. Autom. Control*, vol. 39, no. 6, pp. 1310–1314, Jun. 1994.

[7] I. R. Petersen and D. C. McFarlane, "Optimal guaranteed cost control and filtering for uncertain linear systems," *IEEE Trans. Autom. Control*, vol. 39, no. 9, pp. 1971–1977, Sep. 1994.

[8] D. S. Bernstein and W. M. Haddad, "Steady-state Kalman filtering with an H∞ error bound," in *Proc. Amer. Control Conf.*, 1989, pp. 847–852.

[9] F. Yang, Z. Wang, Y. S. Hung, and H. Shu, "Mixed h/sub 2//H/sub /spl infin// filtering for uncertain systems with regional pole assignment," *IEEE Trans. Aerosp. Electron. Syst.*, vol. 41, no. 2, pp. 438–448, Apr. 2005.

[10] M. A. Gandhi and L. Mili, “Robust Kalman filter based on a generalized maximum-likelihood-type estimator,” *IEEE Trans. Signal Process.*, vol. 58, no. 5, pp. 2509–2520, May 2010.

[11] O. García Crespillo, D. Medina, J. Skaloud, and M. Meurer, “Tightly coupled GNSS/INS integration based on robust M-estimators,” in *Proc. IEEE/ION Position, Location Navigat. Symp.*, 2018, pp. 1554–1561.

[12] J. Rife and D. Gebre-Egziabher, “Symmetric overbounding of correlated errors,” *Navigation*, vol. 54, no. 2, pp. 109–124, 2007.

[13] G. W. Pulford, “A proof of the spherically symmetric overbounding theorem for linear systems,” *J. Inst. Navigat.*, vol. 55, no. 4, pp. 283–292, 2008.

[14] S. E. Langel, S. M. Khanafseh, and B. S. Pervan, “Bounding integrity risk for sequential state estimators with stochastic modeling uncertainty,” *J. Guid., Control, Dyn.*, vol. 37, no. 1, pp. 36–46, 2014, doi: 10.2514/1.62056.

[15] S. Langel, O. García Crespillo, and M. Joerger, “A new approach for modeling correlated Gaussian errors using frequency domain overbounding,” in *Proc. Position, Navigat. Timing Symp.*, 2020, pp. 868–876.

[16] “DO-229D: Minimum operational performance standards for global positioning system/wide area augmenation system airborne equipment,” RTCA, Washington, DC, USA, Tech. Rep. RTCA/SC-159, 2006.

[17] E. Gallon, M. Joerger, S. Perea, and B. Pervan, “Error model development for ARAIM exploiting satellite motion,” in *Proc. 32nd Int. Tech. Meeting Satell. Division Inst. Navigat.*, 2019, pp. 3162–3174.

[18] E. Gallon, M. Joerger, and B. Pervan, “Robust modeling of GNSS tropospheric delay dynamics,” *IEEE Trans. Aerosp. Electron. Syst.*, vol. 57, no. 5, pp. 2992–3003, Oct. 2021.

[19] S. Khanafseh et al., “Multipath error modeling for automotive applications,” in *Proc. 31st Int. Tech. Meeting Satell. Division Inst. Navigat.*, Miami, FL, USA, 2018, pp. 1573–1589.

[20] V. A. Tupysev, O. A. Stepanov, A. V. Loparev, and Y. A. Litvinenko, “Guaranteed estimation in the problems of navigation information processing,” in *Proc. IEEE Control Appl., Intell. Control*, 2009, pp. 1672–1677.

[21] S. Langel, O. García Crespillo, and M. Joerger, “Bounding sequential estimation errors due to Gauss-Markov noise with uncertain parameters,” in *Proc. 32nd Int. Tech. Meeting Satell. Division Inst. Navigat.*, 2019, pp. 3079–3098.

[22] O. García Crespillo, M. Joerger, and S. Langel, “Overbounding GNSS/INS integration with uncertain GNSS Gauss-Markov error parameters,” in *Proc. Position, Navigat. Timing Symp.*, 2020, pp. 481–489.

[23] S. Langel, O. García Crespillo, and M. Joerger, “Overbounding the effect of uncertain Gauss-Markov noise in Kalman filtering,” *Navigation*, vol. 68, no. 2, pp. 259–276, 2021. [Online]. Available: https://onlinelibrary.wiley.com/doi/abs/10.1002/navi.419

[24] R. G. Brown and P. Y. Hwang, *Introduction to Random Signals and Applied Kalman Filtering*, 4th ed. vol. 3. New York, NY, USA: Wiley, 2012.

[25] N. J. Kasdin, “Discrete simulation of colored noise and stochastic processes and 1/f/sup /spl alpha// power law noise generation,” *Proc. IEEE*, vol. 83, no. 5, pp. 802–827, May 1995.

Omar García Crespillo (Member, IEEE) received the M.Sc. (Ing.) degree in telecommunication engineering from the University of Málaga, Málaga, Spain, in 2013, and the Ph.D. degree in robotics, control and intelligent systems from the Swiss Federal Institute of Technology Lausanne (EFPL), Lausanne, Switzerland, in 2022.

He is currently Group Leader with the Navigation Department of the German Aerospace Center (DLR) where he leads activities in GNSS, inertial sensors, integrated navigation systems and integrity monitoring for safe ground and air transportation systems.

Dr. Crespillo was the recipient of the SESAR Young Scientist Award (Ph.D. category) in 2022.

Steve Langel received the Ph.D. degree in mechanical and aerospace engineering from the Illinois Institute of Technology (IIT), Chicago, IL, USA, in 2014.

He is currently a Lead Signal Processing Engineer with The MITRE Corporation, Bedford, MA, USA, focusing on the development of multisensor navigation and fault detection algorithms. His research interests include robust estimation algorithms for safety-critical applications.

Dr. Langel has been a member of the MITRE technical staff since 2014.

Mathieu Joerger (Senior Member, IEEE) received the Diplôme d’Ingenieur (M.S.) degree in mechatronics from the National Institute of Applied Sciences, Strasbourg, France, in 2002, and the M.S. and Ph.D. degrees in mechanical and aerospace engineering from Illinois Institute of Technology (IIT), Chicago, IL, USA, in 2002 and 2009, respectively.

He is currently an Assistant Professor with the Kevin T. Crofton Department of Aerospace and Ocean Engineering, Virginia Tech, Blacksburg, VA, USA. Prior to joining VT, he was an Assistant Professor with the University of Arizona, Tucson, AZ, USA, and a Research Assistant Professor with IIT.

Dr. Joerger is currently the Senior Editor of Navigation for IEEE Transactions on Aerospace and Electronic Systems. He was the recipient of the Institute of Navigation (ION) Bradford Parkinson Award in 2009, and ION Early Achievement Award in 2014.